Pharmaceutical Research, Vol. 26, No. 3, March 2009 (© 2008)
DOI: 10.1007/s11095-008-9802-1

Expert Review

Targeted Delivery with Peptidomimetic Conjugated Self-Assembled Nanoparticles

Esmaiel Jabbari[1,2]

Received October 3, 2008; accepted December 1, 2008; published online December 17, 2008

Abstract. Peptides produce specific nanostructures, making them useful for targeting in biological systems but they have low bioavailability, potential immunogenicity and poor metabolic stability. Peptidomimetic self-assembled NPs can possess biological recognition motifs as well as providing desired engineering properties. Inorganic NPs, coated with self-assembled macromers for stability and anti-fouling, and conjugated with target-specific ligands, are advancing imaging from the anatomy-based level to the molecular level. Ligand conjugated NPs are attractive for cell-selective tumor drug delivery, since this process has high transport capacity as well as ligand dependent cell specificity. Peptidomimetic NPs can provide stronger interaction with surface receptors on tumor cells, resulting in higher uptake and reduced drug resistance. Self-assembled NPs conjugated with peptidomimetic antigens are ideal for sustained presentation of vaccine antigens to dendritic cells and subsequent activation of T cell mediated adaptive immune response. Self-assembled NPs are a viable alternative to encapsulation for sustained delivery of proteins in tissue engineering. Cell penetrating peptides conjugated to NPs are used as intracellular delivery vectors for gene expression and as transfection agents for plasmid delivery. In this work, synthesis, characterization, properties, immunogenicity, and medical applications of peptidomimetic NPs in imaging, tumor delivery, vaccination, tissue engineering, and intracellular delivery are reviewed.

KEY WORDS: conjugation; nanoparticles; peptidomimetic; self-assembly; targeted delivery.

INTRODUCTION

Nanoparticles (NPs) have found broad range of applications in medicine and pharmacy because they are highly effective in overcoming the biological defense system and vascular barriers. These applications include drug and gene delivery (1), growth and differentiation factor delivery in regenerative medicine (2), vaccination (3,4), fluorescent biological labeling (5), detection of proteins and pathogens and probing the DNA structure (6), separation and purification of biological molecules and cells (7), as contrast agents in imaging (8), and for phagokinetic studies (9).

Synthetic macromolecules (polymers) provide great flexibility in the design of NPs and allow the production of a wide range of NPs with varying drug solubility, circulation half-life, particle size, and degradation to fit a particular application (10). NPs with hydrodynamic diameter >400 nm are readily cleared by macrophages of the mononuclear phagocyte system (MPS) while smaller particles with <30 nm diameter can escape from phagocytes and pass through blood vessels with prolonged half-life (11,12). More importantly, NPs produced from synthetic polymers can be stabilized against dissolution, premature degradation, or denaturation in physiological environment by long-range hydrophobic interactions or crosslinking (13). The ability to control the degradation characteristics of synthetic NPs makes them very useful for sustained delivery of therapeutics in medicine and pharmacy (14–32). Although synthetic polymer-based NPs provide enormous flexibility in design, they lack monodispersity in size, shape, morphology, and surface functional groups, which adversely affects their selectivity/specificity in biological applications. In tumor targeting, imaging, and gene delivery success depends on the NPs' ability to target one organelle, cell, or tissue over another. In other words, specificity plays a very important role in reducing side effects or increasing resolution.

Self-assembly refers to the spontaneous formation of higher order structures from simpler building blocks (32). Self-assembly is a process by which complex 3D structures with well-defined functions are built starting from simple building blocks such as short sequences of nucleotides, saccharides, phospholipids, or amino acids (33). Short sequences of amino acids or peptides are especially attractive for self-assembly because nanostructures with varying size, shape, morphology, and surface functional group can be assembled by arranging the 24 naturally occurring amino acids in different sequences or by changing the sequence length (34). For example, the peptide

[1] Biomimetic Materials and Tissue Engineering Laboratory, Department of Chemical Engineering, University of South Carolina, Columbia, South Carolina 29208, USA.
[2] To whom correspondence should be addressed. (e-mail: jabbari@engr.sc.edu)

produced from amino acid sequence EAKA–EAKA–EAKA–EAKA self-assembles into cylinders while the sequence VVVV–VVKK self-assembles into spherical NPs (34). Unlike synthetic polymer-based NPs, peptide self-assembly produces highly specific nanostructures with precisely the same configuration, conformation, size, and functionality, making them very useful for targeting in biological systems (32,33,35). In peptide-based systems, self-assembly takes place by the interplay between three factors: (1) sequestration of non-polar side groups of the peptide chains from aqueous solution, (2) formation of hydrogen bonds and electrostatic interaction within secondary structures of the peptide and loss of interactions with solvent, and (3) extensive van der Waals interactions between the constituent atoms of the peptide. In essence, matching of non-polar patches, patterns of hydrogen and electrostatic interactions, and the formation of buried surfaces within the self-assembled structures are the driving force for self-assembly of peptides (32,33,36). The weak nature of these interactions, compared to covalent bonding in cross-linked networks and ionic bonding in crystalline solids, results in conformational reversibility/plasticity of the interacting components (32,33). As a consequence, highly specific and optimized conformations are produced, which are ideal for recognition in biological systems. It should be mentioned that although these nanostructures are optimized for recognition in biological systems, they are not designed with respect to desired engineering properties such as thermodynamic stability, mechanical properties, and desired dissolution/degradation characteristics.

Peptidomimetic self-assembly is a process to produce nanostructures from synthetic macromolecular chains by mimicking the pattern of weak non-polar, polar, hydrogen bonding, and electrostatic interactions in peptides. Each unique 3D structure of a peptide corresponds to a unique active role in biological systems, thus providing functional specificity (35). However, peptides by themselves have low bioavailability, potential immunogenicity and poor metabolic stability *in vivo* (37). Peptidomimetic self-assembled structures can potentially possess biological recognition motifs as well as desired engineering properties. Furthermore, self-assembled NPs represent a multivalent form of the ligand for interaction with biological receptors, often disposed in clusters (38), resulting in stronger interaction or stimulating particular subsets of receptors (3,39). In the following sections, synthesis, characterization, properties, immunogenicity, and medical applications of peptidomimetic self-assembled NPs are reviewed.

SYNTHESIS AND SELF-ASSEMBLY OF PEPTIDOMIMETIC NPs

Natural colloidal particles like liposomes and lipid-core micelles have been used for NPs preparation (40–42) but they tend to be cleared rapidly from the circulation (43). To improve circulation half-life, natural NPs are PEGylated by covalently linking methoxy-polyethylene glycol (m-PEG) aldehyde to the N-terminal amine group of the protein (Schiffs-base linkage), followed by reduction with sodium borohydride to stabilize the linkage against hydrolysis (44). Natural polymers like gelatin (45), chitosan (46,47), lipids (48) and synthetic polymers like poly(lactide-co-glycolide) (PLGA) (49–51), poly(DL-lactide) (52), poly(ε-caprolactone) (PCL) (53), poly(cyanoacrylate) (54), and poly(β-aminoesters) (55), and their copolymers with hydrophilic polymers like poly (ethylene glycol) (PEG) and poly(vinyl alcohol) (PVA) have been used as biomaterials to produce NPs (28–31,56). Linear and star Poly(L-lactide)-*b*-poly(ethylene oxide) copolymers have been used to produce degradable NPs (28–31,56). The PLA-PEG and PLGA-PEG NPs can be loaded with a variety of bioactive agents while the ethylene oxide (EO) blocks in the copolymer act as a surfactant to stabilize the NPs. However, the EO units impart hydrophilicity to the copolymer, which limits the duration of release of therapeutic agents from the NPs to short-term (1–2 days). PVA-graft-PLGA NPs have been used for local delivery of Paclitaxel in restenosis treatment but an initial burst release dominates the early release profile followed by a slow continuous release of a small fraction of the drug (56). Amino cyclodextrin conjugated PLGA polymers have been used to produce biodegradable NPs as a carrier for delivery of proteins (57).

Natural polymers like chitosan can be PEGylated and functionalized at the distal end for peptide conjugation by reaction with PEG and *N*-hydroxy succinimide (NHS) in the presence of 1-Ethyl-3-[3-dimethylaminopropyl]carbodiimide hydrochloride (EDC) (58). Polymers with hydroxyl end-groups can be succinimide-functionalized by treating with *N*, *N*′-Disuccinimidyl carbonate (DSC) and conjugated with lysine-terminated peptides by the reaction of succinimide end-group of the polymer with amine group of the lysine (59), as shown in reaction scheme a in Fig. 1. Different reaction schemes for conjugation of synthetic polymers/macromers to peptides are shown in Fig. 1. Long-chain polymers like PLGA and PCL, due to their hydrophobic nature, tend to aggregate into micro- and nano-particles with broad particle size distribution (60). PLGA and PCL copolymers with PEG self-assemble in aqueous environment and produce NPs with relatively narrow size distribution, but active agents are released relatively fast (within the first 24 h) from PEGylated PLGA NPs (31). Our laboratory has synthesized hydrophobic poly(lactide fumarate) (PLAF) and amphiphilic poly(lactide-co-ethylene oxide fumarate) (PLEOF) macromers that self-assemble to form degradable NPs. The macromers are synthesized by condensation polymerization of short PLA chains with PEG and fumaryl chloride (61). Carboxylic acid end-groups or fumarate groups along the chain can be used for conjugation of multiple peptides or peptidomimetic sequences to the macromer before self-assembly or to NPs after self-assembly (59). For example, peptides can be conjugated to PLAF and PLEOF by the reaction between amine group of the peptide with carboxylic acid end-group of PLAF/PLEOF in the presence of coupling reagent *N*,*N*′-diisopropylcarbodiimide (DIC) and catalyst *N*,*N*-dimethylaminopyridine (DMAP) [reaction b in Fig. 1). In addition, other peptides can be covalently linked to the macromer by Michael's addition reaction between the unsaturated fumarate groups of the macromer with sulfhydryl group of cysteine-functionalized peptide [reaction c in Fig. 1).

One method to conjugate peptides to macromers is to selectively iodinate the peptide at the N-terminal using nitrite catalysts, followed by the reaction of iodinated peptide with thiol-containing molecules such as *N*-acetylcysteine and glutathione to form peptide conjugates (62) [reaction d in Fig. 1). Peptides with free thiol functionality can be conju-

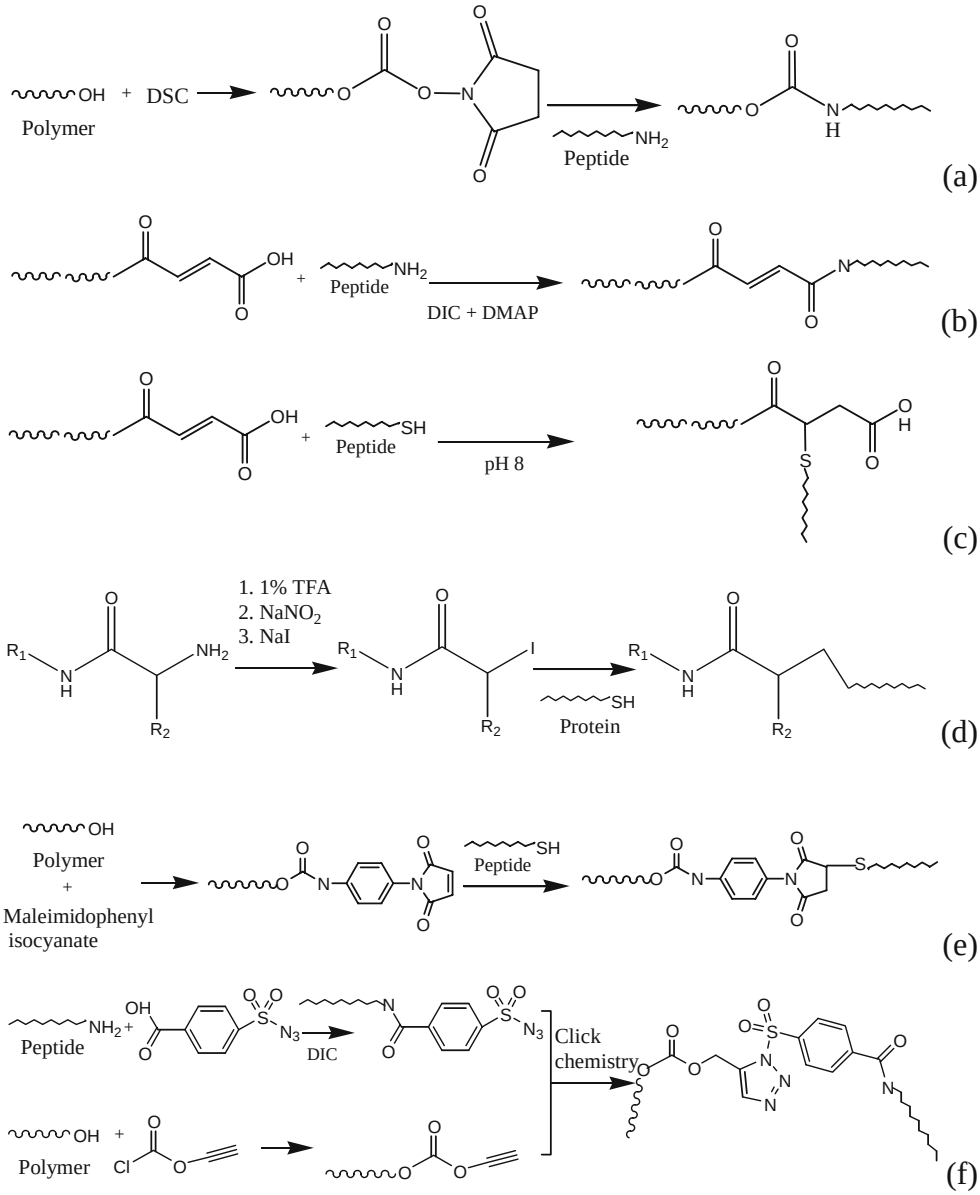

Fig. 1. Conjugation reaction schemes: *a* succinimide-terminated polymer with lysine-terminated peptide; *b* carboxylic acid group of polymer with amine group of peptide; *c* unsaturated group of polymer with sulfhydryl group of cysteine-functionalized peptide; *d* iodine-functionalized polymer with thiol-containing peptide; *e* maleimide-functionalized polymer with thiol-containing peptide; and *f* propargyl-functionalized polymer with azide-functionalized peptide.

gated to synthetic polymers by thiol-maleimide conjugation (63). In this approach, *p*-maleimidophenyl isocyanate is used for functionalization of hydroxyl-terminated polymer (64) [reaction e in Fig. 1). The "click reaction" can also be used for conjugation of peptides to macromers (65,66). In "click reaction", the peptide is functionalized with an azide group by reacting with 4-carboxybenzenesulfonazide while the macromer is functionalized with a propargyl group by reacting with propargyl ester chloride. Next, the peptide is conjugated to the macromer (before or after self-assembly) by "click chemistry" between reactive azide group of the peptide and propargyl group of the macromer [reaction f in Fig. 1).

Recently, regioselectively addressable functionalized template molecules (RAFT), which exhibit two independent and chemically addressable domains, have been used for sequential and regioselective assembly of peptides and biologically functional units (67). By preventing steric hindrance, these templates allow sequential conjugation of multiple peptides to a single molecule to confer biological recognition (68).

CHARACTERIZATION OF PEPTIDOMIMETIC NPs

Peptide conjugated macromers and polymers are the building blocks of peptidomimetic self-assembled NPs. The chemical structure of the synthetic polymer or macromer can be characterized by ^{1}H-NMR and ^{13}C-NMR, and the molecular weight distribution can be characterized by gel permeation

chromatography (GPC) and mass spectrometry. ^{1}H-NMR and ^{13}C-NMR are useful for determining the ratio of monomers incorporated in the polymer chain compared to that in the feed. For example, in the synthesis of amphiphilic PLEOF macromer in which PLA and PEG blocks are linked with fumaryl chloride, presence of peaks at 6.90 ppm in the ^{1}H-NMR spectrum (attributable to the hydrogens of the fumarate group) confirmed the incorporation of fumarate monomers into PLEOF macromer (69). Furthermore, ratio of peaks in the NMR spectrum due to chemical shifts centered at 5.1 ppm (due to the hydrogen attached to methine group of lactide monomer) and 3.6 ppm (due to the methylene hydrogens (–CH2–CH2–O–) of ethylene oxide repeat units) was directly related to the molar ratio of PLA to PEG blocks in the terpolymer (69). For feed PLA molar fractions of 0.06, 0.13, and 0.21, the fraction of PLA incorporated in the terpolymer was 0.037, 0.056, and 0.068, respectively, which demonstrated that the reactivity of PLA with fumaryl chloride was significantly less than that of PEG (69). GPC can be used to determine the optimum polymer or conjugated peptide–polymer conjugate chain length for self-assembly (70). The sequence distribution of the polymer–peptide conjugate can be determined by matrix-assisted laser desorption-ionization time-of-flight (MALDI-TOF) mass spectrometry (71). In MALDI-TOF, sample is vaporized and ionized without fragmentation and a time-of-flight mass analyzer is used to acquire the mass spectra. To sequence the peptide, the molecular ion is fragmented by post-source decay (PSD; for peptides <1,500 Da) or ion-source decay (ISD; for peptides >1,500 Da) and the sequence is determined from the mass of fragmented ions (72). Size exclusion chromatography combined with MALDI mass spectrometry (SEC/MALDI) (73) or pulsed gradient spin-echo (PGSE) NMR combined with MALDI can be used to determine molecular weight distribution of macromers and polymers with very high accuracy (74). Accurate determination of macromer molecular weight distribution and sequence distribution of the conjugated peptide is required for relating the chemical/molecular structure to conformation and nanostructure of the self-assembled polymer–peptide conjugate (75).

The secondary structure of the synthesized peptide and peptide–polymer conjugate can be characterized by circular dichroism (CD) and Fourier Transform Infrared Spectrometry (FTIR) (76). CD and FTIR spectral range of 200–300 nm and 1,500–1,800 cm^{-1}, respectively, are utilized for analysis of secondary structures (76). For example, CD spectral analysis of alanine-rich peptide Ac-K-$[A]_{11}$-KGGY-NH_2 demonstrated that the α-helix content of the self-assembled peptide depended on peptide concentration in water and secondary structure was independent of temperature (76). FTIR spectra of the same peptide in water revealed that the β-sheet structure dominated at higher concentrations (76). The interaction of the polymer chain with conjugated peptide can be studied by X-ray reflectivity as well as CD and FTIR (77,78). Site-specific iodine labeling can be used to determine topology of the peptide within the self-assembled NPs by pinpointing the position of iodine label within NPs (77). For example, X-ray reflectivity and iodine labeling experiments indicated that the model pore-forming aromatic peptide H-$(Phe\text{-}Tyr)_5$-Trp-Trp-OH forms an anti-parallel double-stranded β-helix within double-layer lipid membranes (77).

The effect of amino acid sequence on morphology of the self-assembled peptide and peptide conjugate can be imaged with scanning electron microscopy (SEM), transmission electron microscopy (TEM), and atomic force microscopy (AFM) at micro-, nano-, and angstrom-scale resolution, respectively (79,80). *In vitro* bioactivity of the peptide conjugate is determined by ligand–receptor cell binding assay (81). Two-photon excitation fluorescence cross-correlation spectroscopy (TPE-FCCS) coupled with fluorescence correlation spectroscopy (FCS) can directly measure ligand–receptor binding, rather than monitoring the downstream effects. In this technique, a cross-correlation between fluorescence intensities from two spectrally separate fluorophores is generated when the two detection channels measure synchronous fluorescence fluctuations, which is an indication that the two species are physically linked. Ligand–receptor binding at relatively low concentrations (nanomolar) can be measured with this technique and two or more fluorophores can be excited simultaneously (81). The Kaiser test can be used to quantify the density of peptides conjugated to a substrate (82,83).

In vitro toxicity of self-assembled NPs can be determined by cell count after exposure, and the uptake by macrophage cells can be monitored and quantified by live cell confocal microscopy and flow cytometry (84). For example, confocal microscopy and flow cytometry demonstrated that carboxylic acid-functionalized 20 and 200 nm polystyrene NPs are rapidly taken up by murine macrophage cells with 20 nm NPs being faster and more extensive (84). Infrared imaging is an excellent technique for *in vivo* tracking of NPs in animal models (61). In this technique, a near-infrared dye is encapsulated in self-assembled NPs and the NPs are injected in the animal. Next, the animal is scanned in two infrared channels where one channel is used as reference for normalization of intensities. The intensities are displayed in pseudo colors to show regions of low and high intensity (85). Radioisotope labeling with ^{111}In oxy-quinoline can be used for quantitative determination of *in vivo* biodistribution of NPs (86). For radioisotope labeling, NPs are self-assembled in the presence of ^{111}In labeled oxy-quinoline and the labeled NPs are then injected in the animal. At each time point (between 1 and 24 h), the animal is sacrificed, the radioactivity of vital organs is measured with a gamma scintillation counter, and the counts are reported as percent activity recovered per unit mass of tissue (86).

PROPERTIES OF PEPTIDOMIMETIC SELF-ASSEMBLED NPs

Natural and synthetic polymers provide great flexibility in design and allow the production of a wide range of NPs with varying drug solubility, circulation half-life, particle size and distribution, ligand density, and degradation to fit a particular biomedical application (10). Furthermore, synthetic NPs play a role in peptide presentation, due to their ability to induce enhanced and specific responses to conjugated epitopes. Natural colloidal particles like liposomes and lipid-core micelles have been used for the production of NPs (40–42) but they tend to be cleared rapidly from the circulation (43). Natural polymers like gelatin (45), chitosan (46,47), lipids

(48) and synthetic polymers like PLGA (49–51), poly(DL-lactide) (52), PCL (53), poly(cyanoacrylate) (54), and poly(β-aminoesters) (55) have been used to produce NPs for variety of applications in medicine and pharmacy. We have developed biodegradable blends of poly(lactide-co-glycolide fumarate) and poly(lactide-co-ethylene oxide fumarate) (PLGF/PLEOF) macromers that self-assemble to form biodegradable PEGylated NPs (69,87–89), as shown in Fig. 2. The amphiphilic PLEOF serves as a biodegradable colloid stabilizer during the process of self-assembly. The degree of hydrophilicity, hence their circulation half-life, can be controlled by the molecular weight and fraction of PEG in the macromer. NPs ranging 20–500 nm in size can be produced by varying the ratio of PLGF to PLEOF macromers in the NPs, as shown in Table I. The unsaturated fumarate groups can be used to covalently attach ligands for selective targeting of NPs to a particular cell type. The degradation characteristics of the NPs can be adjusted by the ratio of lactide to glycolide, as shown in Fig. 3 (59). According to this figure, PLAF (100% lactide) NPs lost 60% mass in 2 weeks while PLGF (50:50 lactide/glycolide) NPs lost more than 80% mass during the same time.

The release kinetics of a surrogate molecule 1-(2-pyridylazo)-2-naphthol (PAN) from PLAF and PLGF NPs as a function of incubation time in basal cell culture media is shown in Fig. 4. PLGF NPs, due to lower hydrophobicity and faster degradation, released the encapsulated PAN in 15 days, while PLAF NPs released their content in 28 days. It is noteworthy to mention that PLGF and PLAF NPs completely degraded in 15 and 28 days which demonstrated that the release was dominated by hydrolytic degradation and erosion of the matrix. Release characteristics of high molecular weight PLA and PLGA NPs is by diffusion through a porous matrix while release from PLAF and PLGF NPs, due to low macromer molecular weight and high density of hydrophilic chain ends, is by hydrolytic degradation and matrix erosion.

Self-assembling peptides, when conjugated to synthetic polymer chains, can alter the aggregation process of the conjugated polymers. We have demonstrated that blends of PLAF/PLEOF macromers self-assemble into spherical NPs with size ranging 50–800 nm, as shown in Fig. 5. Interestingly, when the self-assembling peptide EAKA–EAKA–EAKA–EAKA (EAKA16) (34) was conjugated to PLAF macromer and the PLAF-EAKA16/PLEOF blend was self-assembled by dialysis, it drastically reduced NPs size and distribution from 50–800 to 150–400 nm, as shown in Fig. 5. These results demonstrate that peptidomimetic NPs have drastically reduced size distribution compared to that of synthetic PLAF/PLEOF macromers. We speculate that the peptide in PLAF-EAKA16/PLEOF conjugate self-assembles at the interface of the aqueous and PLAF phases to minimize free energy. Characterization of PLAF-EAKA16/PLEOF peptidomimetic NPs is in progress and will be reported in future communications.

Peptidomimetic self-assembled structures are stabilized by hydrophobic interactions, hydrogen bonding, and a host of other noncovalent interactions. Thus, amino acid side groups in the primary structure can dictate secondary structures and preference for a specific shape in peptide aggregates (79). Joshi and Verma have investigated the effect of sequence distribution of phenylalanine (F) and proline (P) in a short tetrapeptide on morphology of the aggregates. They observed by AFM and TEM that FFPP peptides self-assembled into circularly wound structures; PPFF resulted in the formation of long fibers; PFFP resulted in the formation of self-assembled NPs while FPPF, FPFP, and PFPF did not form any resolvable structures (79). Therefore, the ability of short peptides to assemble into specific structures or shape depends strongly on the sequence of amino acids.

Kim and collaborators studied the effect of conjugating glucagon-like peptide-1 (GLP-1) to water soluble poly(*N*-vinyl-2-pyrroridone-co-acrylic acid) copolymer to form peptidomimetic VAPG macromers (90). *In vitro*, VAPG increased insulin secretion by 200% over the control and it lasted for 2 weeks but dose–response curves showed that the effective dose of peptidomimetic VAPG was half of that of native GLP-1. Analysis confirmed that the lower bioactivity of VAPG stemmed from polymer conjugation to N-terminal histidine moieties, which actively participate in binding to GLP-1 receptors, resulting in only 16% of N-terminal histidine remaining intact after the conjugation reaction (90). This study demonstrated that amino acids involved in conjugation reactions can potentially lower the activity of peptidomimetic macromers.

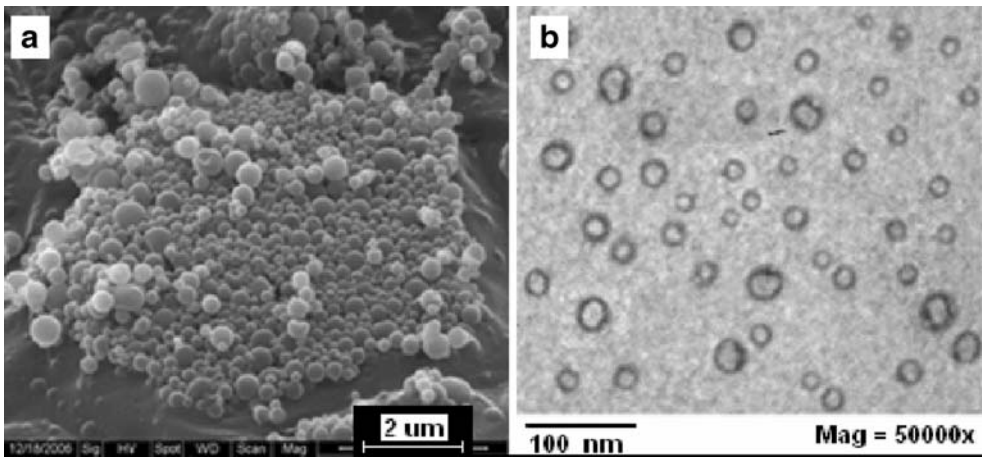

Fig. 2. SEM images of PLGF/PLEOF blends with 90:10 (**a**) and 70:30 (**b**) PLGF/PLEOF ratio, respectively. SEM images demonstrate that NPs size can be changed from 200 to 50 nm by varying PLGF to PLEOF ratio.

Table I. Effect of PLA/PEG Ratio on Number-Average, Volume-Average, and Polydispersity of NPs Produced by Self-Assembly of Biodegradable PLEOF Macromers

PLA/PEG ratio in PLEOF macromer	Number average size (nm)	Volume average size (nm)	Polydispersity index
100:0	480±290	1,630±1,000	3.4
90:10	195±100	670±340	3.4
80:20	50±28	180±100	3.7
60:40	15±6	23±10	1.6

The effect of conjugation of peptide LLEDPVGTVA, derived from a Herpes simplex virus (HSV) glycoprotein, to an oligotuftsin derivative against enzymatic degradation was investigated by Tugyi and collaborators (91). They found that, in human serum, the conjugated peptide provided full protection against enzymatic hydrolysis, while the free peptide was decomposed quickly. Therefore, the selection of carrier significantly influences activity and therapeutic efficiency of peptide mimetic drug candidates. Orzaez and collaborators (92) observed the fusion of a peptidomimetic (peptoid) sequence that inhibited the activity of apoptosome, a macromolecular complex that activates mitochondrial-dependent apoptosis pathways, to cell penetrating peptides significantly affected cell viability. Penetratin-fused peptoid showed higher cell viability and better efficiency as an apoptosis inhibitor than the HIV-1 TAT-fused peptoid (92).

Peptidomimetic sequences have been exploited for design of potent antibacterial agents (93), as potential protease inhibitors (94), as antagonists in protein–protein interactions (95), as modulators of immune system response to provide therapy for auto-immune disorders (96), and as binding agent to transporter proteins in pulmonary transport (97). Studies with antibacterial peptide mimics have demonstrated that activity and selectivity is contingent upon a balance of peptide hydrophobicity and electrostatic charge, rather than any specific receptor–ligand interaction (93). In the case of immunodeficiency virus, the Tat protein, by binding specifically to transactivator response element (TAR), mediates a strong induction for the production of all viral transcripts (98). Athanassiou and collaborators (99), using conformationally constrained beta-hairpin peptidomimetics, have designed a peptidomimetic inhibitor (effective at nanomolar quantities) that binds with high specificity to bovine immunodeficiency virus TAR RNA. Nonspecific signals between pairs of costimulatory molecules are required for full T-cell response in auto-immune disorders. Peptidomimetic NPs that can block signal transduction between pairs of costimulatory molecules are attractive as carriers for suppressing autoimmune diseases mediated by central nervous system-specific T-cells (96). In pulmonary transport, peptidomimetic NPs carrying antibiotic, antiviral, and antineoplastic drugs can bind to high-affinity PEPT2 transporter which is expressed in the respiratory tract epithelium. PEPT2 transporter, which is an integral membrane protein, mediates drug transport by coupling substrate translocation to transmembrane electrochemical proton gradient as the driving force (97).

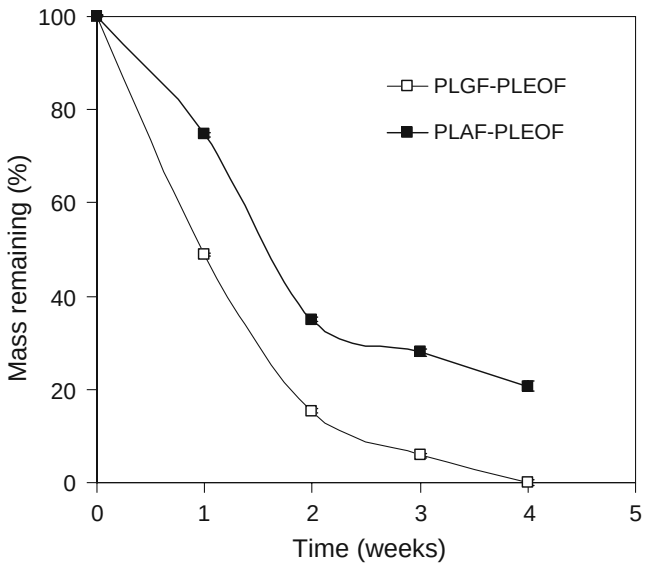

Fig. 3. Degradation characteristics of PLAF (100:0 lactide/glycolide)/PLEOF and PLGF(50:50 lactide/glycolide) NPs with incubation time. PLGF/PLEOF NPs completely degraded in 4 weeks while the more hydrophobic PLAF/PLEOF NPs lost more than 70% of their mass after 4 weeks.

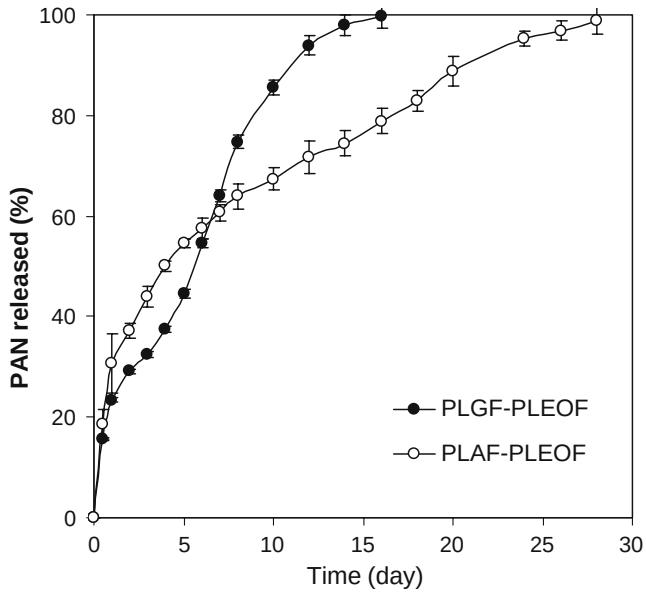

Fig. 4. Cumulative release of PAN from PLAF/PLEOF and PLGF/PLEOF self-assembled NPs with incubation time. PLGF/PLEOF NPs released their content in 2 weeks while PLAF/PLEOF NPs released in 4 weeks.

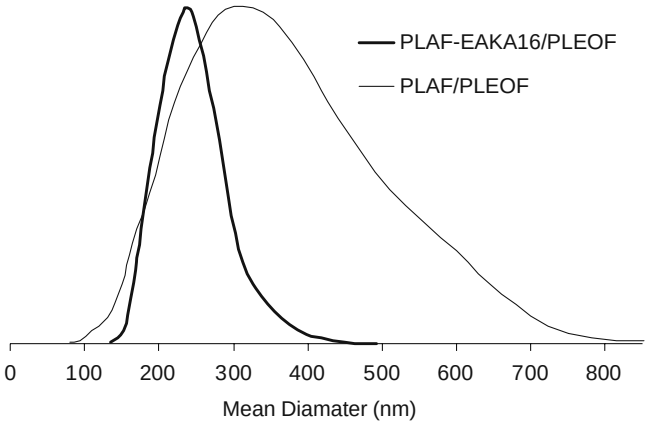

Fig. 5. Size distribution of PLAF/PLEOF NPs with and without conjugation with self-assembling peptide EAKA–EAKA–EAKA–EAKA (EAKA16). PLAF/PLEOF self-assembled NPs without peptide conjugation had 50–800 nm size range while those with conjugation had narrow 150–400 nm size range.

IMMUNOGENICITY OF PEPTIDOMIMETIC NPs

The size, surface charge, surface hydrophilicity (contact angle), surface morphology, the sequence of amino acids of the conjugated peptide, and extent of conjugation of peptidomimetic NPs can significantly affect their immunogenicity and their clearance by the fixed macrophages of the mononuclear phagocytes system (MPS) (100–102). For phagocytosis, particles have to first make contact with the pseudopods of macrophages and be engulfed into the cytoplasm by lamellipods (103). Therefore, hydrophobic and relatively large particles are more susceptible to phagocytosis than hydrophilic ones (104). When relatively large (23 μm average size) albumin spheres were administrated intra-articularly or intramuscularly to rabbits, the spheres were not phagocytosed to an appreciable extent by macrophages within the synovial cavity (105). Studies on phagocytosis of polystyrene, polyacrolein, and cellulose spheres with mouse peritoneal macrophages demonstrate that the sphere size range for maximum phagocytosis is 1–2 μm (102). Furthermore, the extent of phagocytosis increased with increasing zeta potential and it was lowest for particles with zero zeta potential (104). But there was no significant difference in phagocytosis of particles with cationic or anionic surfaces with the same zeta potential value. Based on the results of experiments with cellulose microspheres, least phagocytosis or least susceptibility to immune response was observed with non-ionic hydrophilic surfaces (104). Experiments with cellulose spheres revealed that phagocytosis is enhanced for spheres coated with γ-globulin, fibronectin, gelatin, and tuftsin while albumin reduced phagocytosis (106). The effect of various parameters on phagocytosis of NPs has been studied with polyalkylcyanoacrylate (PACA), polymethylmethacrylate (PMMA), albumin spheres, and poly(lactide-co-glycolide) (PLGA)(103,107–110). These studies show that phagocytosis of particles with 200 nm average size is less than that of 1.5 μm, and phagocytosis of more hydrophobic PMMA NPs is higher than the less hydrophobic PACA (107). Phagocytosis studies with liposomes (naturally-derived nanospheres ranging 10–100 nm in size) showed that, for very small particles, particle adsorption to the macrophage surface is the limiting step (111). Optimal phagocytosis was observed with negatively charged liposomes with 50–100 nm in diameter (111,112). These and other experimental results clearly demonstrate that NPs with high curvature (high surface roughness) with 100–200 size range and surface modified with hydrophilic polymers like poly(ethylene glycol) (PEG) have the best chance to evade the immune system and a prolonged half-life in the circulation (112–116).

Ligands conjugated to NPs can considerably affect immune response and phagocytosis (117,118). Conjugation of ligands that can interact with receptors on macrophages, neutrophils, and natural killer cells can affect phagocytosis and clearance of NPs by MPS (117). These include ligands that interact with Fragment crystallizable (Fc) receptors, complement, fibronectin lipoprotein, mannose, and galactose among other receptors (119–123). For example, mannose-conjugated liposomal NPs had two to four times greater phagocytosis than unconjugated liposomes (124). By the same rationale, due to a variety of non-specific interactions like van der Waals, polar, hydrogen bonding, and electrostatic and any specific interaction, peptidomimetic NPs have greater interaction with immune system components and higher phagocytosis than plain synthetic NPs (117,125). For example, conjugation of a synthetic human chorionic gonadotropin peptide antigen, co-synthesized with a T-cell epitope from tetanus toxoid, to PLGA microspheres induced phagocytosis and enhanced antibody levels relative to soluble peptide or plain PLGA (125). Therefore, peptidomimetic NPs should be modified with non-ionic hydrophilic PEG polymers to reduce their clearance from the circulation by MPS.

APPLICATIONS OF PEPTIDOMIMETIC SELF-ASSEMBLED NPs

Imaging

In the past two decades, molecularly targeted diagnostic and therapeutic agents have dramatically improved cancer diagnosis and treatment. Self-assembled peptide-mimetic polymer micelles are normally used to coat inorganic NPs such as gold, quantum dots, or magnetic iron oxide NPs to target the imaging/diagnostic agent to the intended site (126). Inorganic peptidomimetic NPs, with size in the range of 1–100 nm, can travel through the human body in the blood and lymphatic vessels and identify the desired target by specific biological interactions, such as antibody–antigen (127,128), ligand–receptor interaction (127), nucleic acid hybridization (129), and gene expression (130,131).

Inorganic NPs, coated with self-assembled amphiphilic macromers and conjugated with multiple peptidomimetic target-specific ligands provide the possibility for imaging with multiple techniques or combining multiple functionalities (132). The most promising synthetic magnetic nanoparticle (MNP) as diagnostic agent, superparamagnetic iron oxide NPs (SPION) with mean diameter of 30 nm, has several advantages over traditional contrast agents including lower toxicity, stronger enhancement of proton relaxation, and lower detection limit (126). MNPs are biologically safe as they are metabolized into elemental iron species by either hydrolytic enzymes or the acidic conditions found inside lysosomes. The iron is then merged in normal body stores and

is subsequently incorporated in hemoglobin (133). To improve colloidal stability and biocompatibility, MNPs are coated with self-assembled amphiphilic macromers such as PEG-phospholipids, poly(maleic anhydride-alt-1-octadecene)-PEG block copolymers (134), polystyrene-poly(acrylic acid) (PS-PAA) block copolymer (135), or degradable polylactide-PEG block copolymer (136). MNPs can be further stabilized structurally by crosslinking with a small molecule ligand such as 2,3-dimercaptosuccinic acid (DMSA) (13). This bifunctional ligand provides structural stability by disulfide cross-linkages between the ligands and the remaining free thiol groups can be used for bioconjugation.

In addition to coating with self-assembled macromers, MNPs are conjugated with peptidomimetic ligands for targeted imaging of a specific cell type or malignant tissue. These include ligands that target α3 integrin receptors on glioblastoma cells (85), CXCR-4 receptors on HIV infected cells and tumor cells (137), peripheral benzodiazepine receptors for imaging traumatic brain injury (138), vesicular monoamine transporter-2 for imaging pancreatic beta-cell mass (139), cannabinoid receptors for neuroinflammation imaging (140), peroxisome proliferator-activated receptor for imaging metabolic and inflammatory disease (141), Sigma receptors for prostate cancer imaging (142), translocator protein for tumor imaging (143), and serotonin transporter receptor for imaging midbrain of patients with depression (144). Inorganic NPs, coated with self-assembled macromers for stability and anti-fouling and conjugated with target-specific ligands, are advancing imaging from the anatomy-based level to the molecular level (145).

Tumor Delivery

One of the most exciting applications of NPs is in targeted tumor delivery (38,146,147). Although diagnosing cancer at an early stage can significantly improve survival rate, novel nanoscale technologies that can selectively target and destroy tumor cells while leaving normal cells unharmed, will reduce patient suffering and recovery time. Chemotherapy is limited by the toxicity of the antitumor drug to healthy tissues (148). Additionally, short circulation half-life in plasma, limited aqueous solubility, and non-selectivity has limited the use of anticancer drugs to more invasive and localized methods, like the use of catheters for chemotherapy or surgery to remove tumor followed by chemotherapy. Intravenous or intraperitoneal administration of antitumor drugs can improve patient compliance and allow targeted delivery to tumor vasculature but these less invasive systemic methods are limited by non-selectivity of antitumor drugs to normal cells and drug resistance in the tumor microenvironment. The absence of selectivity causes intense undesired side effects, thus reducing therapeutic efficacy of the drug (149).

One strategy to circumvent the short half-life and limited solubility and improve selectivity is to encapsulate the antitumor drug in NPs as a carrier and administer the suspension systemically (intravenous injection) (150). NPs provide the opportunity to selectively target the tumor over normal tissue (14–17,151). Tumor blood vessels present several abnormalities compared with normal vessels resulting in enhanced permeation and retention effect (EPR effect) (152–154). The pore cutoff size of most tumor models is 200–400 nm and NPs with diameter <200 nm are selectively taken up by tumor tissue (11,12). However, the association of cytotoxic drugs with NPs modifies the drug biodistribution profile, because untreated NPs are rapidly opsonized and massively cleared (the mean half-life of untreated NPs is 3–5 min after intravenous injection) by the fixed macrophages of the mononuclear phagocytes system (MPS) (100,101). It has been demonstrated that NPs with high curvature (50< diameter<200 nm) and surface modified with hydrophilic PEG polymers have prolonged half-life in the circulation system, leading to the development of long-circulating NPs for delivery of antitumor drugs (113–116). Furthermore, most tumors lack lymph vessels and higher interstitial fluid pressure than normal tissues (due to higher rigidity of the tumor tissue, denser network of collagen fibers, and higher number of fibroblasts which exert increased tension between the fibers), so interstitial fluid and soluble macromolecules are inefficiently removed (17,155). Therefore, there is accumulation of NPs in the interstitium (EPR effect) which retards their additional uptake from the blood vessels to tumor interstitial space, unless the NPs degrade to molecular weights below 50 kDa (156,157). NPs that are modified with ligands that preferentially interact with cell surface receptors on tumor cells improve selectivity and increase the residence time of NPs in the tumor tissue (158). Ligand conjugated NPs are very attractive as a mechanism for cell-selective tumor drug delivery, since this process has high transport capacity as well as ligand dependent cell specificity (159).

The effectiveness of NPs for tumor drug delivery depends, to a great extent, on the selection of ligands that bind with high specificity/affinity to localize the NPs to the tumor environment (160). Many cell surface receptors including folate receptor (161,162), transferrin receptor (163), interleukin-1 (IL-1) receptor (164), epidermal growth factor (EGF) receptor (165), endogenous G-protein coupled receptor (166,167), vasoactive intestinal receptor (gastrointestinal tumor) (168), gastrin and cholecystokinin/gastrin (thyroid and prostate tumor) receptors (169,170), neurotensin receptor (171), vascular endothelial growth factor receptor (172), fibroblast growth factor receptor (173), and $\alpha_v\beta_3$ integrin-binding receptors (158,174,175) have been explored for selective targeting of drug-loaded NPs to tumor cells.

Among these receptors, several synthetic RGD-based peptides have shown high affinity for $\alpha_v\beta_3$ integrin receptor (158,175). This integrin mediates the attachment of cells to the extracellular matrix, is implicated in tumor-induced angiogenesis, tumor invasion, and metastasis, and is upregulated on both cancer cells and tumor-associated blood vessels (176,177). This integrin is present at low levels on most normal tissues (178). Furthermore, it is well established that ligands conjugated to PEGylated NPs display a much higher apparent affinity to cell surface receptors than the free ligand (38,146,147). In essence, NPs represent a multivalent form of the ligand and cell surface receptors are often disposed in clusters (38). As a result, ligand conjugated NPs can potentially provide stronger interaction with surface receptors on tumor cells and tumor blood vessels, resulting in higher drug uptake and reduced drug resistance.

Our laboratory has developed novel PLGF/PLEOF macromers that self-assemble to form biodegradable PEGy-

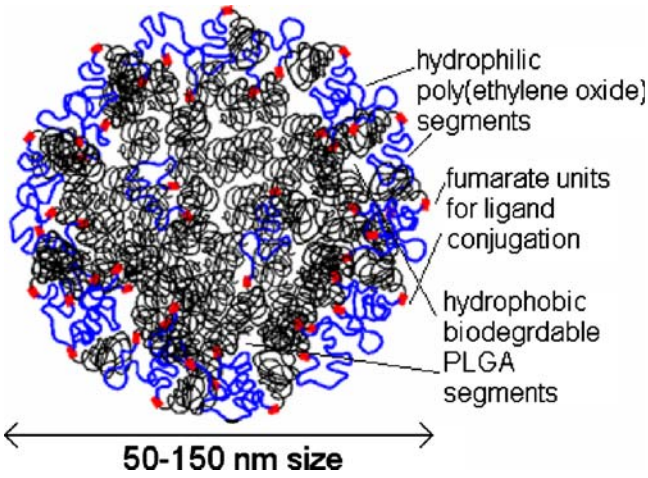

Fig. 6. Schematic diagram of the NPs self-assembled from PLGF/PLEOF blends.

lated NPs (69,87–89), as shown in Fig. 6. The unsaturated fumarate groups of PLGF and PLEOF can be used to covalently attach peptidomimetic ligands with high affinity for tumor cells to the NPs. The linear D-Phe-Cys-Arg-Gly-Asp peptide was synthesized using Fmoc-chemistry (179) and cyclized directly in the solid-phase by coupling the carboxylate group of aspartic acid to the amine group on phenylalanine in the peptide sequence. The cyclic c(–GRGfC–) peptide was conjugated to the NPs and purified by dialysis. The conjugated NPs were incubated with MCF-7 (low $\alpha_v\beta_3$ expression) and U87MG (high $\alpha_v\beta_3$ integrin expression) for 2 h and imaged by fluorescent microscopy. Fig. 7a and b show the confocal fluorescent image of MCF-7 and U87MG cells, respectively. The bright dots in Fig. 7b and their absence in Fig. 7a are the FITC-stained c(–GRGfC–) peptide conjugated NPs that are attached/taken up by U87MG cells that have high expression of $\alpha_v\beta_3$ integrin receptor. Fig. 7c shows the white light image of the conjugated NPs (small white spheres) coupled with the fluorescent image of the U87MG cell (blue). The images in Fig. 7 demonstrate that the c(–GRGfC–) conjugated NPs bind selectively to tumor cells which have high expression of $\alpha_v\beta_3$ integrin receptor.

Although the use of targeted NP delivery systems have significantly improved the survival rate of cancer patients and reduced patient suffering, intense side effects due to uptake by normal tissues, are still a major obstacle to patient compliance in chemotherapy (180). A promising approach to eliminate the toxic side-effects of chemotherapeutic agents, is the use of prodrugs that are activated by cytokines and proteases in the tumor microenvironment (181). For example, conjugation of *N*-butoxycarbonyl-Ala-Ala-Asp-Leu (*N*-BuCa-AADL), a relatively short peptide which is cleaved by Legumain endopeptidase in tumor microenvironment, to Doxorubicin (Dox) produces a prodrug (*N*-BuCa-AADL-Dox) with significantly increased dose of active Dox in breast tumor microenvironment with little accumulation in other tissues (182–186). Legumain (187) is the only asparaginyl endopeptidase of the mammalian genome which is highly expressed by neoplastic, stromal, and endothelial cells in solid tumors (188). Legumain is present on the cell surface and intracellularly in tumor cells and tumor-associated cells in the tumor microenvironment (189,190). Protease-activated prodrugs increase tumor uptake of the active drug, but tumor eradication is limited by the lipophilic character of the prodrug and small molecular size, leading to short circulation half-life and rapid clearance, and ultimately to low dose differential between the tumor and normal tissue. Protease-activated prodrugs encapsulated in self-assembled biodegradable NPs that bind with high affinity to tumor and tumor-associated cells through peptidomimetic ligands provide the potential to eliminate harmful side effects while increasing the efficacy of chemotherapy (see Fig. 8).

Vaccination

Advances in molecular basis of antigen recognition has resulted in the development of rationally designed antigen

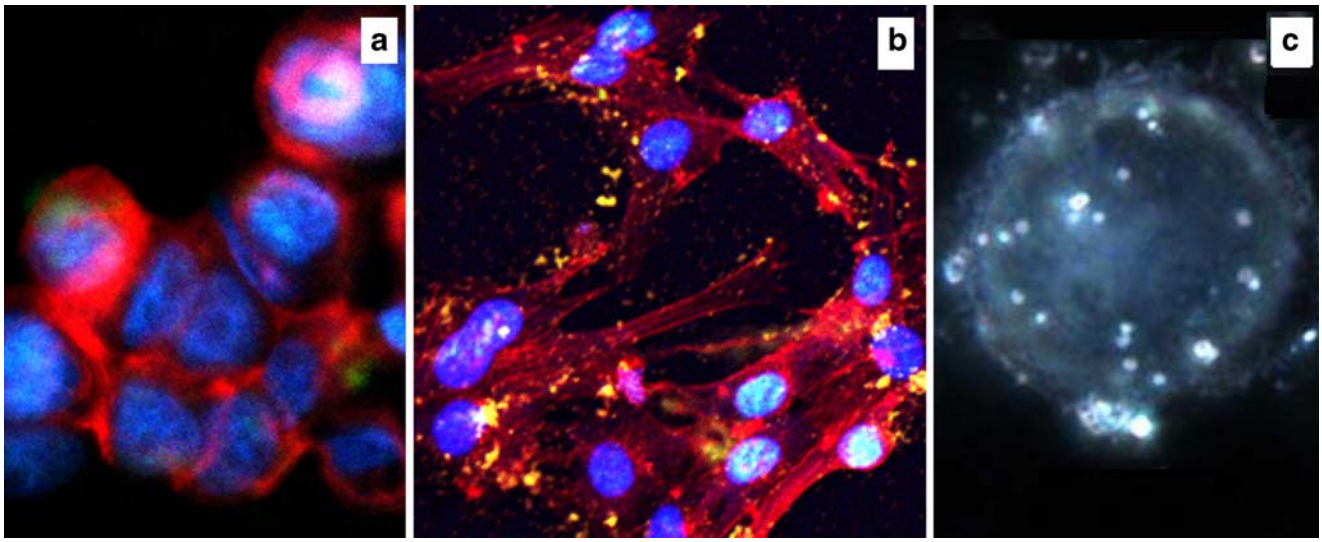

Fig. 7. Fluorescent images of MCF-7 (**a**; low $\alpha_v\beta_3$ integrin expression) and U87MG (**b**; high $\alpha_v\beta_3$ integrin expression) cells. The bright dots in **b** are the FITC-stained peptide conjugated NPs. **c** The white light image of the conjugated NPs (*small white spheres*) coupled with fluorescent image of the cell (*blue*).

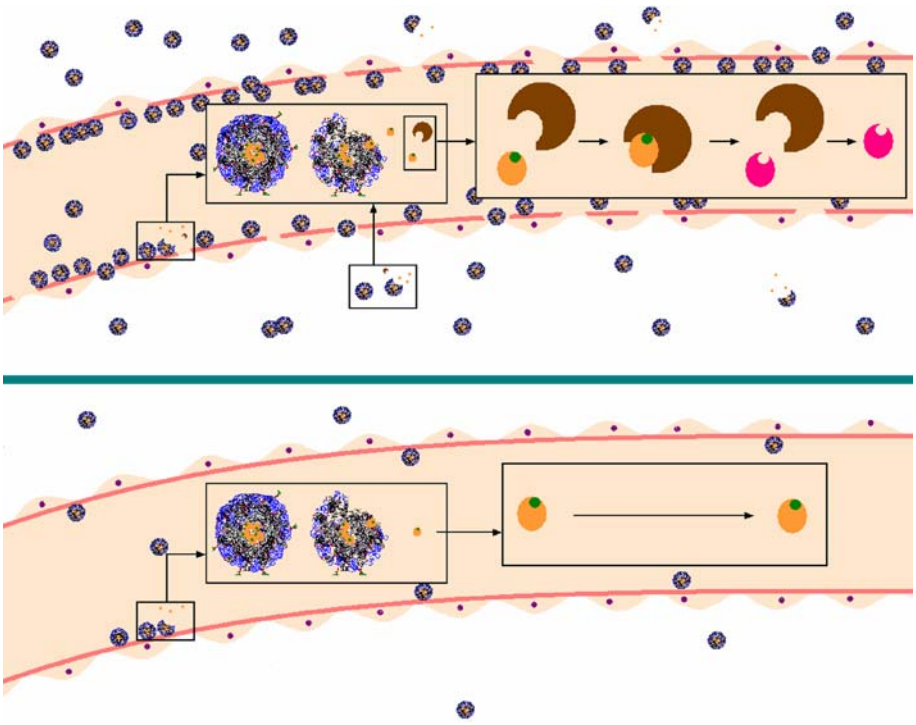

Fig. 8. After systemic administration, prodrug-loaded conjugated NPs are selectively taken up by tumor microvessels (*panel A*) at higher dose compared to normal tissue (*panel B*). After uptake, NPs degrade during the chemotherapy schedule to release the inactive Legumain-activated-Dox prodrug. The prodrug is activated to doxorubicin (*magenta*) by the action of legumain endopeptidase which is highly expressed in the tumor microenvironment. The combination of targeted delivery with conjugated NPs and the use of prodrugs, activated by protease specific to tumor microenvironment, ensure high therapeutic efficiency to eradicate tumor while leaving normal cells unharmed.

specific vaccines based on motifs predicted to bind to human class I and class II major histocompatibility molecules (MHC) (191). Peptide-based vaccines, in which small peptides derived from target proteins (epitopes) are used to provoke an immune reaction, are very attractive for treating infectious diseases and destruction of cancerous cells by the patient's own immune system (192). Synthetic peptides or peptidomimetic sequences for vaccination offer chemical stability, lack of infectious potential, and better manipulation of the immune response through the use of epitopes designed for stimulating a particular subsets of T cells (3). Furthermore, peptidomimetic vaccines are effective in generating immune response to self-proteins by responding to subdominant epitopes (39). Since antibodies can respond to multiple small epitopes on antigens, multi-specific antigen recognition by antibodies and T-cells should be employed for strong immunogenic response (193). An ideal anti-tumor vaccine should incorporate B cell, $CD4^+$, and $CD8^+$ T cell epitopes to ensure both humoral and cellular eradication of tumors (194) and be delivered with potent external immunoadjuvants for strong immune response (195).

For vaccination against HIV, synthetic combination of peptide antigens are amenable to modification to improve immunogenicity and reactivity to multiple virus subtypes (196). The synthetic peptide vaccine containing seven relevant hepatitis C virus (HCV) T-cell epitopes and the T helper cell adjuvant poly-L-arginine induced HCV-specific immunogenic response in a subset of nonresponder patients (197). In another study, vaccination with peptides derived from human vascular endothelial growth factor receptor-2 (VEGFR-2) induced cytotoxic T lymphocytes with potent cytotoxicity against endothelial cell expressing VEGFR-2 (198).

Marazuela and collaborators demonstrated that intranasal delivery of PLGA microspheres containing the peptide with major T-cell epitope of the allergen for olive pollen is effective in preventing subsequent allergic sensitization (199). Renaudet and collaborators have designed and synthesized a self-adjuvanting multivalent glycolipopeptide (GLP) vaccine against cancer containing four components on a molecular delivery system. These components included a) a cluster of tumor-associated carbohydrate antigen (TACA) B-cell epitope, b) a $CD4^+$ T-helper epitope, c) a $CD8^+$ cytotoxic T-cell epitope, and d) a palmitic acid immunoadjuvant (68).

Oil-based incomplete Freund s-type formulations, influenza virosomes (200), aluminum based, and saponins have been used as adjuvants to improve antigen half-life and promote direct entry of peptides into MHC complexes to stimulate T-cell responses (201,202). Although these adjuvants enhance the immune response, there are several disadvantages associated with their use including severity of local tissue irritation, longer duration of the inflammatory reaction at the injection site, minimal induction of cell-

mediated immunity, and eliciting undesirable immunoglobulin E (IgE) responses (203). Microspheres have been used as encapsulation matrix for sustained delivery of peptide antigens and co-encapsulation with other cytokines (204–206). Encapsulation of peptidomimetic antigens in PLGA microspheres significantly enhanced the duration of antigen presentation by dendritic cells (DC) and potency of DC-based vaccination (207). However, microsphere-based delivery is limited by low effective surface area and surface curvature for presentation of multivalent antigens to MHC.

Peptidomimetic self-adjuvant NPs are the ideal carrier for vaccination because they provide large surface area with high curvature for antigen presentation along with sustained delivery of multivalent peptides by conjugation. For example, administration of influenza antigen in chitosan NPs induced higher immune response and significant IgA levels compared to that of free antigen (208). In another study, a vaccine based on PLGA NPs co-encapsulating the poorly immunogenic melanoma antigen along with toll-like receptor ligand, showed immunostimulatory milieu in the tumor microenvironment, evidenced by increased level of pro-inflammatory cytokines compared to the free antigen (208). subcutaneous immunization of mice with poly(γ-glutamic acid) (γ-PGA) NPs entrapping ovalbumin (OVA) efficiently delivered antigenic proteins to antigen presenting cells and more effectively inhibited the growth of OVA-transfected tumors than that of emulsified OVA (209). In addition, γ-PGA NPs did not induce histopathologic changes after subcutaneous injection or acute toxicity through intravenous injection.

For ideal vaccination, the antigens have to be presented by the most efficient antigen presenting dendritic cells that activate a particular subset of T cells and initiate antigen-specific immune response. A rational way of improving the potency and safety of new and already existing vaccines could be to direct vaccines specifically to DCs. Self-assembled NPs conjugated with peptidomimetic antigens are ideal for uptake and sustained presentation of vaccine antigens to dendritic cells and subsequent activation of T cell mediated adaptive immune response. Upon activation, T helper (Th) lymphocytes ($CD4^+$) orchestrate an immune response, augmented with cytolytic T lymphocytes (CTL) or killer T lymphocytes ($CD8^+$), which stimulate the innate immune mechanisms involving natural killer cells and macrophages (210).

Tissue Engineering

Growth and differentiation factors and homing agents play a central role in modulation and control of cell migration, differentiation and maturation, and morphogenesis (211). In particular, bone morphogenetic protein-2 plays a major role in initiating the cascade of chemotaxis, differentiation of marrow stromal cells, and bone regeneration (212). *Recombinant human* bone morphogenetic protein-2 (*rh*BMP-2) is used as the differentiation factor in tissue engineered (TE) scaffolds for bone regeneration and it is used clinically for spinal fusion (213).

BMPs are a group of proteins involved in the development of a wide range of organs and tissues from embryonic through adult stages (214) and they play important roles in tissue repair and remodeling processes after injury (215). In-vivo, BMPs signaling is highly regulated by restricted expression (216), binding peptides (217), proBMP domains (218) and other factors that synergistically enhance the effect of BMPs (219). Therefore, four to five orders of magnitude higher than the amount found endogenously (1 mg/mL for rhBMP-2) have to be loaded in the graft to induce bone formation (215). Such high doses cause adverse effects such as bony overgrowth and immunological reactions (220). We (221) and others (9) have immobilized rhBMP-2 in degradable microspheres but the encapsulated protein has low bioactivity and the release characteristics are less than optimal, adversely affecting the safety profile of rhBMP-2 for clinical applications (222). When rhBMP-2 is delivered in a collagen or PLGA sponge, a large fraction of the protein is lost in the process of irrigating the wound, by the action of antibiotics in the first 24 h after surgical placement, and by soft tissue compression.

Our laboratory has exploited the self-assembly of a novel amphiphilic poly(lactide-co-ethylene oxide fumarate) (PLEOF) macromer in aqueous solution to encapsulate rhBMP-2 and retain its bioactivity. In the process, the protein and PLEOF macromer are dissolved in aqueous solution at physiological conditions. Next, rhBMP-2 is encapsulated by self-assembly of the macromer into NPs (average diameter of 25–75 nm) upon lowering the solution temperature below the macromer critical phase transition, as illustrated in Fig. 9. The PLA units of the macromer allow sustained release of the protein for up to 5 days while PEG units provide stability and prevent protein denaturation. The fumarate units provide sites for covalent attachment and immobilization of the NPs in the TE scaffold for skeletal regeneration. The released rhBMP-2 protein from the NPs had >95% bioactivity and the released protein induced differentiation of bone marrow stromal cells *in vitro*. These results demonstrate that self-assembled NPs are a viable alternative to double emulsion encapsulation for sustained *in situ* delivery and their immobilization in TE scaffolds.

Intracellular Targeting

NPs due to their large surface area, relative to their volume, and high curvature are taken up by cells through the process of endocytosis (223). Pinocytosis or endocytosis of solutes and NPs can occur by four mechanisms including macropinocytosis (non-selective bulk fluid-phase uptake) (224), clathrin-mediated endocytosis (receptor-mediated by clathrin-coated pits on the cell membrane) (225), caveolae-mediated endocytosis (receptor-mediated by caveolae or lipid rafts) (226), and non-receptor-mediated endocytosis (227). Receptor-mediated endocytosis can increase the cellular uptake of NPs by 1,000 times, compared to receptor-independent pathways (228). Due to negative charge of the cell membrane, cationic core/shell NPs self-assembled from biodegradable, cationic and amphiphilic copolymers have been used for intracellular delivery of

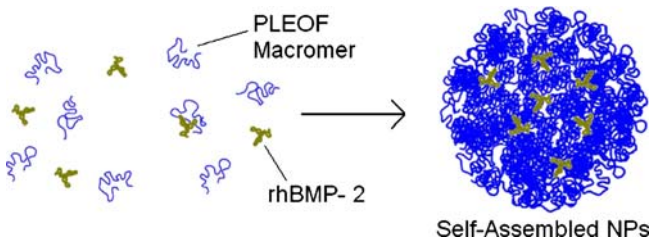

Fig. 9. Schematic diagram illustrating the self-assembly of rhBMP-2 protein with PLEOF macromer in aqueous environment.

anticancer glycoproteins (137). Folate receptors, which are overexpressed on tumor cells, are used for intracellular delivery to cancer cells. For example, when PLGA NPs were coated with a cationic di-block copolymer conjugate, poly(L-lysine)-PEG-folate (PLL-PEG-FOL), the coated NPs had far greater extent of cellular uptake by tumor cells (229). After endocytosis, NPs enter mildly acidic endosomes (pH 5.0–6.5) followed by entry into the degrading environment of lysosomes with significantly lower pH (230). NPs conjugated with fusogenic synthetic peptides like WEAALAEALAEALAEHLAEALAEALEALAA (GALA) or WEAKLAKALAKALAKHLAKALAK–ALKACEA (KALA) has been used for endo-/lysosomal escape of NPs (231).

A new approach for transport of NPs across the cell membrane and into cytosol is by conjugating the NPs with cell penetrating peptides (CPPs) (232). The CPPs include transactivating transcriptor (Tat), Antennapedia (Antp), polyarginine peptides, transportan, and penetratin (232–234). Different size cargo molecules ranging from small molecules to proteins and even liposomes and particles can be delivered by CPPs (235). Due to their ability to penetrate cellular lipid bilayers, CPPs conjugated to NPs are used as delivery vectors for gene expression such as oligonucleotides for antisense, siRNA and dsDNA, and as transfection agents for plasmid delivery (236). Conjugation of HIV-1 Tat cell penetrating peptide to polyethyleneimine PEI/DNA nanocomplexes improved cellular uptake of gene vectors and enhanced gene transfection efficiency of neurons up to 14-fold (237).

CONCLUSIONS

Peptidomimetic self-assembled NPs have a wide range of applications in medicine and pharmacy. These applications include molecular imaging, tumor targeting, gene delivery, growth factor delivery in regenerative medicine, biological labeling, detection of proteins and pathogens and probing the DNA structure, separation and purification of biological molecules and cells. NPs, due to their size, are highly effective in overcoming the biological defense system and vascular barriers. In biological applications, success of NPs depends on their ability to target one organelle, cell, or tissue over another. Selectivity and specificity play a very important role in reducing side effects or increasing resolution. Self-assembly refers to the spontaneous formation of higher order structures from simpler building blocks. Peptidomimetic self-assembly is a process to produce nanostructures from synthetic macromolecular chains by mimicking the pattern of weak non-polar, polar, hydrogen bonding, and electrostatic interactions in peptides. Each unique 3D structure of a peptide corresponds to a unique active role in biological systems, thus providing functional specificity. In this review, synthesis, characterization, properties, and immunogenicity of peptide-conjugated self-assembled NPs are reviewed. The most important and clinically relevant applications of peptidomimetic self-assembled NPs for molecular imaging, tumor targeting, vaccination, *in situ* protein delivery, and intracellular delivery are reviewed.

ACKNOWLEDGEMENTS

This publication was made possible in part by NIH Grant No. P20 RR-016461 from the National Center for Research Resources and by National Science Foundation/EPSCoR under Grant No. 2001 RII-EPS-0132573. This work was also supported by a grant to E. Jabbari from National Science Foundation under Grant No. CBET-0756394. The author thanks Dr. Xuezhong He and Angel E. Mercado for the assistance in the preparation of this manuscript.

REFERENCES

1. D. Pantarotto, C. D. Partidos, J. Hoebeke, F. Brown, E. Kramer, J. P. Briand, S. Muller, M. Prato, and A. Bianco. Immunization with peptide-functionalized carbon nanotubes enhances virus-specific neutralizing antibody responses. *Chem. Biol*. **10**(10):961–966 (2003). doi:10.1016/j.chembiol.2003.09.011.
2. T. Sasaki, N. Iwasaki, K. Kohno, M. Kishimoto, T. Majima, S. I. Nishimura, and A. Minami. Magnetic nanoparticles for improving cell invasion in tissue engineering. *J. Biomed. Mater. Res. A*. **86A**(4):969–978 (2008). doi:10.1002/jbm.a.31724.
3. T. Nagata, T. Aoshi, M. Uchijima, and Y. Koide. *In vivo* hierarchy of individual T-cell epitope-specific helper T-cell subset against an intracellular bacterium. *Vaccine*. **26**(40):5123–5127 (2008). doi:10.1016/j.vaccine.2008.03.061.
4. S. P. Wang, N. Mamedova, N. A. Kotov, W. Chen, and J. J. Studer. Antigen/antibody immunocomplex from CdTe nanoparticle bioconjugates. *Nano Lett*. **2**(8):817–822 (2002). doi:10.1021/nl0255193.
5. J. M. Nam, C. S. Thaxton, and C. A. Mirkin. Nanoparticle-based bio-bar codes for the ultrasensitive detection of proteins. *Science*. **301**(5641):1884–1886 (2003). doi:10.1126/science.1088755.
6. R. Mahtab, J. P. Rogers, and C. J. Murphy. Protein-sized quantum-dot luminescence can distinguish between straight, bent, and kinked oligonucleotides. *J. Am. Chem. Soc*. **117**(35):9099–9100 (1995). doi:10.1021/ja00140a040.
7. Y. Jing, L. R. Moore, P. S. Williams, J. J. Chalmers, S. S. Farag, B. Bolwell, and M. Zborowski. Blood progenitor cell separation from clinical leukapheresis product by magnetic nanoparticle binding and magnetophoresis. *Biotechnol. Bioeng*. **96**(6):1139–1154 (2007). doi:10.1002/bit.21202.
8. X. Montet, R. Weissleder, and L. Josephson. Imaging pancreatic cancer with a peptide–nanoparticle conjugate targeted to normal pancreas. *Bioconj. Chem*. **17**(4):905–911 (2006). doi:10.1021/bc060035+.
9. W. J. Parak, R. Boudreau, M. Le Gros, D. Gerion, D. Zanchet, C. M. Micheel, S. C. Williams, A. P. Alivisatos, and C. Larabell. Cell motility and metastatic potential studies based on quantum dot imaging of phagokinetic tracks. *Adv. Mater*. **14**(12):882–885 (2002). doi:10.1002/1521-4095(20020618)14:12<882::AID-ADMA882>3.0.CO;2-Y.
10. M. J. Vicent, and R. Duncan. Polymer conjugates: nanosized medicines for treating cancer. *Trends Biotechnol*. **24**(1):39–47 (2006). doi:10.1016/j.tibtech.2005.11.006.
11. S. K. Hobbs, W. L. Monsky, F. Yuan, W. G. Roberts, L. Griffith, V. P. Torchilin, and R. K. Jain. Regulation of transport pathways in tumor vessels: role of tumor type and microenvironment. *Proc. Natl. Acad. Sci. USA*. **95**(8):4607–4612 (1998). doi:10.1073/pnas.95.8.4607.
12. S. Unezaki, K. Maruyama, J. Hosoda, I. Nagae, Y. Koyanagi, M. Nakata, O. Ishida, M. Iwatsuru, and S. Tsuchiya. Direct measurement of the extravasation of polyethyleneglycol-coated liposomes into solid tumor tissue by *in vivo* fluorescence microscopy. *Int. J. Pharmaceut*. **144**(1):11–17 (1996). doi:10.1016/S0378-5173(96)04674-1.
13. J. H. Lee, Y. M. Huh, Y. Jun, J. Seo, J. Jang, H. T. Song, S. Kim, E. J. Cho, H. G. Yoon, J. S. Suh, and J. Cheon. Artificially engineered magnetic nanoparticles for ultra-sensitive molecular imaging. *Nat. Med*. **13**(1):95–99 (2007). doi:10.1038/nm1467.
14. N. Nishiyama, and K. Kataoka. Current state, achievements, and future prospects of polymeric micelles as nanocarriers for drug and gene delivery. *Pharmacol. Ther*. **112**(3):630–648 (2006). doi:10.1016/j.pharmthera.2006.05.006.
15. C. Vauthier, C. Dubernet, C. Chauvierre, I. Brigger, and P. Couvreur. Drug delivery to resistant tumors: the potential of

poly(alkyl cyanoacrylate) nanoparticles. *J. Contr. Rel.* **93** (2):151–160 (2003). doi:10.1016/j.jconrel.2003.08.005.
16. Y. Kato, H. Onishi, and Y. Machida. Application of chitin and chitosan derivatives in the pharmaceutical field. *Curr. Pharm. Biotechnol.* **4–5**:303–309 (2003). doi:10.2174/1389201033489748.
17. I. Brigger, C. Dubernet, and P. Couvreur. Nanoparticles in cancer therapy and diagnosis. *Adv. Drug Del. Rev.* **54**(5):631–651 (2002). doi:10.1016/S0169-409X(02)00044-3.
18. P. S. Kumar, T. R. Saini, D. Chandrasekar, V. K. Yellepeddi, S. Ramakrishna, and P. V. Diwan. Novel approach for delivery of insulin loaded poly(lactide-co-glycolide) nanoparticles using a combination of stabilizers. *Drug Delivery.* **14**(8):517–523 (2007). doi:10.1080/10717540701606467.
19. A. Basarkar, D. Devineni, R. Palaniappan, and J. Singh. Preparation, characterization, cytotoxicity and transfection efficiency of poly (DL-lactide-co-glycolide) and poly(DL-lactic acid) cationic nanoparticles for controlled delivery of plasmid DNA. *Int. J. Pharmaceut.* **343**(1–2):247–254 (2007). doi:10.1016/j.ijpharm.2007.05.023.
20. F. Tewes, E. Munnier, B. Antoon, L. N. Okassa, S. Cohen-Jonathan, H. Marchais, L. Douziech-Eyrolles, M. Souce, P. Dubois, and I. Chourpa. Comparative study of doxorubicin-loaded poly(lactide-co-glycolide) nanoparticles prepared by single and double emulsion methods. *Euro. J. Pharm. Biopharm.* **66**(3):488–492 (2007). doi:10.1016/j.ejpb.2007.02.016.
21. P. Kallinteri, S. Higgins, G. A. Hutcheon, C. B. St Pourcain, and M. C. Garnett. Novel functionalized biodegradable polymers for nanoparticle drug delivery systems. *Biomacromolecules.* **6** (4):1885–1894 (2005). doi:10.1021/bm049200j.
22. E. Leo, B. Brina, F. Forni, and M. A. Vandelli. *In vitro* evaluation of PLA nanoparticles containing a lipophilic rug in water-soluble or insoluble form. *Int. J. Pharmaceut.* **278**(1):133–141 (2004). doi:10.1016/j.ijpharm.2004.03.002.
23. H. J. Jeon, J. I. Jeong, M. K. Jang, Y. H. Park, and J. W. Nah. Effect of solvent on the preparation of surfactant-free poly(DL-lactide-co-glycolide) nanoparticles and norfloxacin release characteristics. *Int. J. Pharmaceut.* **207**(1–2):99–108 (2000). doi:10.1016/S0378-5173(00)00537-8.
24. E. Jabbari, A. Florschutz, L. Petersen, N. Liu, L. Lu, B. Currier, and M. Yaszemski. Release characteristics of recombinant human bone morphogenic protein-2 from PLGA microspheres embedded in a poly(propylene fumarate) porous scaffold. *Trans. Soc. Biomaterials* 512 (2004).
25. A. Lamprecht, N. Ubrich, H. Yamamoto, U. Schafer, H. Takeuchi, C. M. Lehr, P. Maincent, and Y. Kawashima. Design of rolipram-loaded nanoparticles: comparison of two preparation methods. *J. Contr. Rel.* **71**(3):297–306 (2001). doi:10.1016/S0168-3659(01)00230-9.
26. S. K. Sahoo, J. Panyam, S. Prabha, and V. Labhasetwar. Residual polyvinyl alcohol associated with poly (D,L-lactide-co-glycolide) nanoparticles affects their physical properties and cellular uptake. *J. Contr. Rel.* **82**(1):105–114 (2002). doi:10.1016/S0168-3659(02)00127-X.
27. S. Sant, M. Thommes, and P. Hildgen. Microporous structure and drug release kinetics of polymeric nanoparticles. *Langmuir.* **24**(1):280–287 (2008). doi:10.1021/la702244w.
28. Q. Liu, C. Cai, and C. Dong. Poly(L-lactide)-*b*-poly(ethylene oxide) copolymers with different arms: hydrophilicity, biodegradable nanoparticles, *in vitro* degradation, and drug-release behavior. *J. Biomed. Mater. Res. A* 2008, in press.
29. J. Lee, E. Cho, and K. Cho. Incorporation and release behavior of hydrophobic drug in functionalized poly(D,L-lactide)-block-poly(ethylene oxide) micelles. *J. Contr. Rel.* **94**(2–3):323–335 (2004). doi:10.1016/j.jconrel.2003.10.012.
30. G. Katsikogianni, and K. Avgoustakis. Poly(lactide-co-glycolide)-methoxy-poly(ethylene glycol) nanoparticles: drug loading and release properties. *J. Nanosci. Nanotech.* **6**(9–10):3080–3086 (2006). doi:10.1166/jnn.2006.404.
31. K. Avgoustakis. Pegylated poly(lactide) and poly(lactide-co-glycolide) nanoparticles: preparation, properties and possible applications in drug delivery. *Curr. Drug Del.* **1**(1):321–333 (2004). doi:10.2174/1567201043334605.
32. J. A. Thomas. Locking self-assembly: strategies and outcomes. *Chem. Soc. Rev.* **36**(6):856–868 (2007). doi:10.1039/b415246h.
33. G. Colombo, P. Soto, and E. Gazit. Peptide self-assembly at the nanoscale: a challenging target for computational and experimental biotechnology. *Trends Biotechnol.* **25**(5):211–218 (2007). doi:10.1016/j.tibtech.2007.03.004.
34. Y. S. Hong, R. L. Legge, S. Zhang, and P. Chen. Effect of amino acid sequence and pH on nanofiber formation of self-assembling peptides EAK16-II and EAK16-IV. *Biomacromolecules.* **4** (5):1433–1442 (2003). doi:10.1021/bm0341374.
35. J. A. Patch, and A. E. Barron. Mimicry of bioactive peptides via non-natural, sequence-specific peptidomimetic oligomers. *Curr. Opin. Chem. Biol.* **6**(6):872–877 (2002). doi:10.1016/S1367-5931(02)00385-X.
36. J. A. R. Worrall, M. Górna, X. Y. Pei, D. R. Spring, R. L. Nicholson, and B. F. Luisi. Design and chance in the self-assembly of macromolecules. *Biochem. Soc. Trans.* **35**:502–507 (2007). doi:10.1042/BST0350502.
37. P. W. Latham. Therapeutic peptides revisited. *Nat. Biotechnol.* **17**(8):755–757 (1999). doi:10.1038/11686.
38. E. A. Rossi, R. M. Sharkey, W. McBride, H. Karacay, L. Zeng, H. J. Hansen, D. M. Goldenberg, and C. H. Chang. Development of new multivalent-bispecific agents for pretargeting tumor localization and therapy. *Clin. Cancer Res.* **9** (10):3886S–3896S (2003).
39. S. Bacsi, R. Geoffrey, G. Visentin, R. De Palma, R. Aster, and J. Gorski. Identification of T cells responding to a self-protein modified by an external agent. *Hum. Immunol.* **62**(2):113–124 (2001). doi:10.1016/S0198-8859(00)00242-1.
40. T. A. Elbayoumi, S. Pabba, A. Roby, and V. P. Torchilin. Antinucleosome antibody-modified liposomes and lipid-core micelles for tumor-targeted delivery of therapeutic and diagnostic agents. *J. Liposome Res.* **17**(1):1–14 (2007). doi:10.1080/08982100601186474.
41. Y. Gupta, A. Jain, P. Jain, and S. K. Jain. Design and development of folate appended liposomes for enhanced delivery of 5-FU to tumor cells. *J. Drug Target.* **15**(3):231–240 (2007). doi:10.1080/10611860701289719.
42. S. D. Li, and L. Huang. Surface-modified LPD nanoparticles for tumor targeting. *Oligonucl. Therapeutics.* **1082**:1–8 (2006).
43. K. J. Harrington, M. Mubashar, and A. M. Peters. Polyethylene glycol in the design of tumor-targetting radiolabelled macromolecules—lessons from liposomes and monoclonal antibodies. *Quart. J. Nucl. Med.* **46**(3):171–180 (2002).
44. J. M. Harris, and R. B. Chess. Effect of pegylation on pharmaceuticals. *Nat. Rev. Drug Discov.* **2**(3):214–221 (2003). doi:10.1038/nrd1033.
45. G. Y. Lee, K. Park, J. H. Nam, S. Y. Kim, and Y. Byun. Anti-tumor and anti-metastatic effects of gelatin-doxorubicin and PEGylated gelatin-doxorubicin nanoparticles in SCC7 bearing mice. *J. Drug Target.* **14**(10):707–716 (2006). doi:10.1080/10611860600935701.
46. Y. W. Cho, S. A. Park, T. H. Han, D. H. Son, J. S. Park, S. J. Oh, D. H. Moon, K. J. Cho, C. H. Ahn, Y. Byun, I. S. Kim, I. C. Kwon, and S. Y. Kim. *In vivo* tumor targeting and radionuclide imaging with self-assembled nanoparticles: mechanisms, key factors, and their implications. *Biomaterials.* **28**(6):1236–1247 (2007). doi:10.1016/j.biomaterials.2006.10.002.
47. J. H. Park, S. Kwon, M. Lee, H. Chung, J. H. Kim, Y. S. Kim, R. W. Park, I. S. Kim, S. B. Seo, I. C. Kwon, and S. Y. Jeong. Self-assembled nanoparticles based on glycol chitosan bearing hydrophobic moieties as carriers for doxorubicin: *in vivo* biodistribution and anti-tumor activity. *Biomaterials.* **27**(1):119–126 (2006). doi:10.1016/j.biomaterials.2005.05.028.
48. L. H. Reddy, R. K. Sharma, K. Chuttani, A. K. Mishra, and R. S. R. Murthy. Influence of administration route on tumor uptake and biodistribution of etoposide loaded solid lipid nanoparticles in Dalton's lymphoma tumor bearing mice. *J. Contr. Rel.* **105**(3):185–198 (2005). doi:10.1016/j.jconrel.2005.02.028.
49. C. M. Solbrig, J. K. Saucier-Sawyer, V. Cody, W. M. Saltzman, and D. J. Hanlon. Polymer nanoparticles for immunotherapy from encapsulated tumor-associated antigens and whole tumor cells. *Mol. Pharm.* **4**(1):47–57 (2007). doi:10.1021/mp060107e.
50. A. S. Yang, L. Yang, W. Liu, Z. Y. Li, H. B. Xu, and X. L. Yang. Tumor necrosis factor alpha blocking peptide loaded PEG-PLGA nanoparticles: preparation and *in vitro* evaluation. *Int. J. Pharmaceut.* **331**(1):123–132 (2007). doi:10.1016/j.ijpharm.2006.09.015.
51. L. Nobs, F. Buchegger, R. Gurny, and E. Allemann. Biodegradable nanoparticles for direct or two-step tumor

immunotargeting. *Bioconj. Chem.* **17**(1):139–145 (2006). doi:10.1021/bc050137k.
52. A. Cirstoiu-Hapca, L. Bossy-Nobs, F. Buchegger, R. Gurny, and F. Delie. Differential tumor cell targeting of anti-HER2 (Herceptin (R)) and anti-CD20 (Mabthera (R)) coupled nanoparticles. *Int. J. Pharmaceut.* **331**(2):190–196 (2007). doi:10.1016/j.ijpharm.2006.12.002.
53. J. S. Chawla, and M. M. Amiji. Biodegradable poly(epsilon-caprolactone) nanoparticles for tumor-targeted delivery of tamoxifen. *Int. J. Pharmaceut.* **249**(1–2):127–138 (2002). doi:10.1016/S0378-5173(02)00483-0.
54. M. Y. Simeonova, and M. N. Antcheva. Effect of farmorubicin both free and associated with poly(butylcyanoacrylate) nanoparticles on phagocytic and NK activity of peritoneal exudate cells from tumor-bearing mice. *J. Drug Target.* **15**(4):302–310 (2007). doi:10.1080/10611860701349844.
55. H. Devalapally, D. Shenoy, S. Little, R. Langer, and M. Amiji. Poly(ethylene oxide)-modified poly(beta-amino ester) nanoparticles as a pH-sensitive system for tumor-targeted delivery of hydrophobic drugs: part 3. Therapeutic efficacy and safety studies in ovarian cancer xenograft model. *Cancer Chemother. Pharmacol.* **59**(4):477–484 (2007). doi:10.1007/s00280-006-0287-5.
56. U. Westedt, M. Kalinowski, M. Wittmar, T. Merdan, F. Unger, J. Fuchs, S. Schaller, U. Bakowsky, and T. Kissel. Poly(vinyl alcohol)-graft-poly(lactide-co-glycolide) nanoparticles for local delivery of paclitaxel for restenosis treatment. *J. Contr. Rel.* **119**(1):41–51 (2007). doi:10.1016/j.jconrel.2007.01.009.
57. H. Gao, Y. N. Wang, Y. G. Fan, and J. B. Ma. Conjugates of poly(DL-lactide-co-glycolide) on amino cyclodextrins and their nanoparticles as protein delivery system. *J. Biomed. Mater. Res. A*. **80A**(1):111–122 (2007). doi:10.1002/jbm.a.30861.
58. E. Fernandez-Megia, R. Novoa-Carballal, E. Quinoa, and R. Riguera. Conjugation of bioactive ligands to PEG-grafted chitosan at the distal end of PEG. *Biomacromolecules*. **8**(3):833–842 (2007). doi:10.1021/bm060889x.
59. A. E. Mercado, X. He, W. Xu, and E. Jabbari. Release characteristics of a model protein from self-assembled succinimide-terminated poly(lactide-co-glycolide ethylene oxide fumarate) nanoparticles. *Nanotechnology* 2008, in press.
60. F. Esmaeili, M. H. Ghahremani, B. Esmaeili, M. R. Khoshayand, F. Atyabi, and R. Dinarvand. PLGA nanoparticles of different surface properties: preparation and evaluation of their body distribution. *Int. J. Pharmaceut.* **349**(1–2):249–255 (2008). doi:10.1016/j.ijpharm.2007.07.038.
61. X. He, J. Ma, A. E. Mercado, W. Xu, and E. Jabbari. Cytotoxicity of paclitaxel in biodegradable self-assembled core-shell poly(lactide-co-glycolide ethylene oxide fumarate) nanoparticles. *Pharm. Res.* **25**:1552–1562 (2008). doi:10.1007/s11095-007-9513-z.
62. H. T. Deng. Nitrite-assisted peptide iodination and conjugation. *J. Pept. Sci.* **13**(2):107–112 (2007). doi:10.1002/psc.806.
63. M. E. Gindy, S. Ji, T. R. Hoye, A. Z. Panagiotopoulos, and R. K. Prud'homme. Preparation of poly(ethylene glycol) protected nanoparticles with variable bioconjugate ligand density. *Biomacromolecules*. **9**:2705–2711 (2008).
64. K. Ananda, P. Nacharaju, P. K. Smith, S. A. Acharya, and B. N. Manjula. Analysis of functionalization of methoxy-PEG as maleimide-PEG. *Anal. Biochem.* **374**(2):231–242 (2008). doi:10.1016/j.ab.2007.11.034.
65. D. A. Ossipov, and J. Hilborn. Poly(vinyl alcohol)-based hydrogels formed by "click chemistry". *Macromolecules*. **39**(5):1709–1718 (2006). doi:10.1021/ma052545p.
66. Q. Wang, T. R. Chan, R. Hilgraf, V. V. Fokin, K. B. Sharpless, and M. G. Finn. Bioconjugation by copper(I)-catalyzed azide-alkyne [3 + 2] cycloaddition. *J. Am. Chem. Soc.* **125**(11):3192–3193 (2003). doi:10.1021/ja021381e.
67. D. Boturyn, J. L. Coll, E. Garanger, M. C. Favrot, and P. Dumy. Template assembled cyclopeptides as multimeric system for integrin targeting and endocytosis. *J. Am. Chem. Soc.* **126**(18):5730–5739 (2004). doi:10.1021/ja049926n.
68. O. Renaudet, L. BenMohamed, G. Dasgupta, I. Bettahi, and P. Dumy. Towards a self-adjuvanting multivalent B and T cell epitope containing synthetic glycolipopeptide cancer vaccine. *ChemMedChem*. **3**(5):737–741 (2008). doi:10.1002/cmdc.200700315.
69. X. He, and E. Jabbari. Material properties and cytocompatibility of injectable MMP degradable poly(lactide ethylene oxide fumarate) hydrogel as a carrier for marrow stromal cells. *Biomacromolecules*. **8**(3):780–792 (2007). doi:10.1021/bm060671a.
70. Y. Wang, C. Y. Ke, C. W. Beh, S. Q. Liu, S. H. Goh, and Y. Y. Yang. The self-assembly of biodegradable cationic polymer micelles as vectors for gene transfection. *Biomaterials*. **28**(35):5358–5368 (2007). doi:10.1016/j.biomaterials.2007.08.013.
71. K. Stuhler, and H. E. Meyer. MALDI: more than peptide mass fingerprints. *Curr. Opin. Mol. Ther.* **6**(3):239–248 (2004).
72. L. J. Li, R. W. Garden, and J. V. Sweedler. Single-cell MALDI: a new tool for direct peptide profiling. *Trends Biotechnol.* **18**(4):151–160 (2000). doi:10.1016/S0167-7799(00)01427-X.
73. H. Sato, N. Ichieda, H. Tao, and H. Ohtani. Data processing method for the determination of accurate molecular weight distribution of polymers by SEC/MALDI-MS. *Anal. Sci.* **20**(9):1289–1294 (2004). doi:10.2116/analsci.20.1289.
74. M. Mazarin, S. Viel, B. Allard-Breton, A. Thevand, and L. Charles. Use of pulsed gradient spin-echo NMR as a tool in MALDI method development for polymer molecular weight determination. *Anal. Chem.* **78**(8):2758–2764 (2006). doi:10.1021/ac0522207.
75. H. Dong, S. E. Paramonov, L. Aulisa, E. L. Bakota, and J. D. Hartgerink. Self-assembly of multidomain peptides: balancing molecular frustration controls conformation and nanostructure. *J. Am. Chem. Soc.* **129**(41):12468–12472 (2007). doi:10.1021/ja072536r.
76. K. Baginska, J. Makowska, W. Wiczk, F. Kasprzykowski, and L. Chmurzynski. Conformational studies of alanine-rich peptide using CD and FTIR spectroscopy. *J. Pept. Sci.* **14**(3):283–289 (2008). doi:10.1002/psc.923.
77. A. Kusel, Z. Khattari, P. E. Schneggenburger, A. Banerjee, T. Salditt, and U. Diederichsen. Conformation and interaction of a D,L-alternating peptide with a bilayer membrane: X-ray reflectivity, CD, and FTIR spectroscopy. *ChemPhysChem*. **8**(16):2336–2343 (2007). doi:10.1002/cphc.200700477.
78. D. Krikorian, A. Stavrakoudis, N. Biris, C. Sakarellos, D. Andreu, E. de Oliveira, G. Mezo, Z. Majer, F. Hudecz, S. Welling-Wester, M. T. Cung, and V. Tsikaris. Influence of sequential oligopeptide carriers on the bioactive structure of conjugated epitopes: comparative study of the conformation of a Herpes simplex virus glycoprotein gD-1 epitope in the free and conjugated form, and protein "built-in" crystal structure. *Biopolymers*. **84**(4):383–399 (2006). doi:10.1002/bip.20486.
79. K. B. Joshi, and S. Verma. Sequence shuffle controls morphological consequences in a self-assembling tetrapeptide. *J. Pept. Sci.* **14**(2):118–126 (2008). doi:10.1002/psc.955.
80. B. B. Hole, J. A. Schwarz, J. L. Gilbert, and B. L. Atkinson. A study of biologically active peptide sequences (P-15) on the surface of an ABM scaffold (PepGen P-15 (TM)) using AFM and FTIR. *J. Biomed. Mater. Res. A*. **74A**(4):712–721 (2005). doi:10.1002/jbm.a.30331.
81. J. L. Swift, M. C. Burger, D. Massotte, T. E. S. Dahms, and D. T. Cramb. Two-photon excitation fluorescence cross-correlation assay for ligand–receptor binding: cell membrane nanopatches containing the human mu-opioid receptor. *Anal. Chem.* **79**(17):6783–6791 (2007). doi:10.1021/ac0709495.
82. B. Li, J. X. Chen, and J. H. C. Wang. RGD peptide-conjugated poly(dimethylsiloxane) promotes adhesion, proliferation, and collagen secretion of human fibroblasts. *J. Biomed. Mater. Res. A*. **79A**(4):989–998 (2006). doi:10.1002/jbm.a.30847.
83. Y. Ito, M. Kajihara, and Y. Imanishi. Materials for enhancing cell-adhesion by immobilization of cell-adhesive peptide. *J. Biomed. Mater. Res. A*. **25**(11):1325–1337 (1991). doi:10.1002/jbm.820251102.
84. M. J. Clift, B. Rothen-Rutishauser, D. M. Brown, R. Duffin, K. Donaldson, L. Proudfoot, K. Guy, and V. Stone. The impact of different nanoparticle surface chemistry and size on uptake and toxicity in a murine macrophage cell line. *Toxicol. Appl. Pharmacol.* **232**:418–427 (2008).
85. W. Xiao, N. Yao, L. Peng, R. H. Liu, and K. S. Lam. Near-infrared optical imaging in glioblastoma xenograft with ligand-targeting alpha3 integrin. *Eur. J. Nucl. Med. Mol. Imag.*, 2008, in press.
86. D. Shenoy, S. Little, R. Langer, and M. Amiji. Poly(ethylene oxide)-modified poly(beta-amino ester) nanoparticles as a pH-

sensitive system for tumor-targeted delivery of hydrophobic drugs: part 2. *In vivo* distribution and tumor localization studies. *Pharm. Res*. **22**(12):2107–2114 (2005). doi:10.1007/s11095-005-8343-0.
87. E. Jabbari, and X. He. Synthesis and characterization of bioresorbable *in situ* crosslinkable ultra low molecular weight poly(lactide) macromer. *J. Mater. Sci.—Mater. Med*. **19**(1):311–318 (2008). doi:10.1007/s10856-006-0020-2.
88. E. Jabbari. Self-assembly and nanoparticle formation of a novel bioresorbable and crosslinkable terpolymer. Proceed. AIChE Ann. Meeting, 2006: 324f.
89. E. Jabbari, W. Xu, and X. He, Degradation characteristics of novel *in-situ* crosslinkable poly(lactide-co-glycolide-ethylene oxide-fumarate) copolymer networks. *Trans. Soc. Biomater.* 353 (2007).
90. S. Kim, and Y. H. Bae. Long-term insulinotropic activity of glucagon-like peptide-1/polymer conjugate on islet microcapsules. *Tissue Eng. A*. **10**(11–12):1607–1616 (2004). doi:10.1089/ten.2004.10.1607.
91. R. Tugyi, G. Mezo, S. Gitta, E. Fellinger, D. Andreu, and F. Hudecz. Effect of conjugation with polypeptide carrier on the enzymatic degradation of Herpes simplex virus glycoprotein D derived epitope peptide. *Bioconj. Chem*. **19**(8):1652–1659 (2008). doi:10.1021/bc700469r.
92. M. Orzaez, L. Mondragon, I. Marzo, G. Sanclimens, A. Messeguer, E. Perez-Paya, and M. J. Vicent. Conjugation of a novel Apaf-1 inhibitor to peptide-based cell-membrane transporters: effective methods to improve inhibition of mitochondria-mediated apoptosis. *Peptides*. **28**(5):958–968 (2007). doi:10.1016/j.peptides.2007.02.014.
93. B. Bechinger. Structure and functions of channel-forming peptides: magainins, cecropins, melittin and alamethicin. *J. Membr. Biol.* **156**(3):197–211 (1997). doi:10.1007/s002329900201.
94. G. Fear, S. Komarnytsky, and I. Raskin. Protease inhibitors and their peptidomimetic derivatives as potential drugs. *Pharmacol. Ther.* **113**(2):354–368 (2007). doi:10.1016/j.pharmthera.2006.09.001.
95. L. O. Sillerud, and R. S. Larson. Design and structure of peptide and peptidomimetic antagonists of protein–protein interaction. *Curr. Protein Peptide Sci*. **6**(2):151–169 (2005). doi:10.2174/1389203053545462.
96. S. D. Allen, S. V. Rawale, C. C. Whitacre, and P. T. P. Kaumaya. Therapeutic peptidomimetic strategies for autoimmune diseases: costimulation blockade. *J. Pept. Res*. **65**(6):591–604 (2005). doi:10.1111/j.1399-3011.2005.00256.x.
97. D. A. Groneberg, A. Fischer, K. F. Chung, and H. Daniel. Molecular mechanisms of pulmonary peptidomimetic drug and peptide transport. *Am. J. Respir. Cell Mol. Biol*. **30**(3):251–260 (2004). doi:10.1165/rcmb.2003-0315TR.
98. J. T. Randolph, and D. A. DeGoey. Peptidomimetic inhibitors of HIV protease. *Curr. Top. Med. Chem*. **4**(10):1079–1095 (2004). doi:10.2174/1568026043388330.
99. Z. Athanassiou, K. Patora, R. L. A. Dias, K. Moehle, J. A. Robinson, and G. Varani. Structure-guided peptidomimetic design leads to nanomolar beta-hairpin inhibitors of the Tat-TAR interaction of bovine immunodeficiency virus. *Biochemistry*. **46**(3):741–751 (2007). doi:10.1021/bi0619371.
100. D. E. Owens, and N. A. Peppas. Opsonization, biodistribution, and pharmacokinetics of polymeric nanoparticles. *Int. J. Pharmaceut*. **307**(1):93–102 (2006). doi:10.1016/j.ijpharm.2005.10.010.
101. R. FernandezUrrusuno, E. Fattal, J. M. Rodrigues, J. Feger, P. Bedossa, and P. Couvreur. Effect of polymeric nanoparticle administration on the clearance activity of the mononuclear phagocyte system in mice. *J. Biomed. Mater. Res. A*. **31**(3):401–408 (1996). doi:10.1002/(SICI)1097-4636(199607)31:3<401::AID-JBM15>3.0.CO;2-L.
102. F. L. Ahsan, I. P. Rivas, M. A. Khan, and A. I. T. Suarez. Targeting to macrophages: role of physicochemical properties of particulate carriers—liposomes and microspheres—on the phagocytosis by macrophages. *J. Contr. Rel*. **79**(1–3):29–40 (2002). doi:10.1016/S0168-3659(01)00549-1.
103. V. Schafer, H. V. Briesen, H. Rubsamen-Waigmann, A. M. Steffan, C. Royer, and J. Kreuter. Phagocytosis and degradation of human serum albumin microspheres and nanoparticles in human macrophages. *J. Microencaps*. **11**:261–269 (1994). doi:10.3109/02652049409040455.
104. Y. Tabata, and Y. Ikada. Effect of surface wettability of microspheres on phagocytosis. *J. Colloid Interface Sci*. **127** (1):132–140 (1989). doi:10.1016/0021-9797(89)90013-1.
105. D. J. Burgess, and S. S. Davis. Potential use of albumin microspheres as a drug delivery system: II. *In vivo* deposition and release of steroids. *Int. J. Pharmaceut*. **46**(1–2):69–76 (1988). doi:10.1016/0378-5173(88)90011-7.
106. Y. Ikada, and Y. Tabata. Phagocytosis of bioactive microspheres. *J. Bioact. Compat. Polym*. **1**:32–46 (1986). doi:10.1177/088391158600100104.
107. V. Schafer, H. Vonbriesen, R. Andreesen, A. M. Steffan, C. Royer, S. Troster, J. Kreuter, and H. Rubsamenwaigmann. Phagocytosis of nanoparticles by human-immunodeficiency-virus (HIV)-infected macrophages—a possibility for antiviral drug targeting. *Pharm. Res*. **9**(4):541–546 (1992). doi:10.1023/A:1015852732512.
108. A. Rolland, G. Merdrignac, J. Gouranton, D. Bourel, R. Leverge, and B. Genetet. Flow cytometric quantitative-evaluation of phagocytosis by human mononuclear and polymorphonuclear cells using fluorescent nanoparticles. *J. Immunol. Methods*. **96** (2):185–193 (1987). doi:10.1016/0022-1759(87)90313-9.
109. R. A. Bejjani, D. BenEzra, J. L. L. Bourges, S. Gautier, M. Halhal, D. Chauvaud, R. Gurny, and F. F. Behar-Cohen. Phagocytosis of polylactides (PLA) nanoparticles by bovine and human RPE cells *in vitro*. *Invest. Ophthalmol. Vis. Sci*. **43**: U518–U518 (2002).
110. K. D. Newman, P. Elamanchili, G. S. Kwon, and J. Samuel. Uptake of poly(D,L-lactic-co-glycolic acid) microspheres by antigen-presenting cells *in vivo*. *J. Biomed. Mater. Res. A*. **60** (3):480–486 (2002). doi:10.1002/jbm.10019.
111. A. Raz, C. Bucana, W. E. Fogler, G. Poste, and I. J. Fidler. Biochemical, morphological, and ultrastructural studies on the uptake of liposomes by murine macrophages. *Cancer Res*. **41** (2):487–494 (1981).
112. W. Yan and L. Huang. The effects of salt on the physicochemical properties and immunogenicity of protein based vaccine formulated in cationic liposome. *Int. J. Pharmaceut.* 2008, in press.
113. M. Cegnar, J. Kristl, and J. Kos. Nanoscale polymer carriers to deliver chemotherapeutic agents to tumours. *Expert Opin. Biol. Ther.* **5**(12):1557–1569 (2005). doi:10.1517/14712598.5.12.1557.
114. S. Kommareddy, S. B. Tiwari, and M. M. Amiji. Long-circulating polymeric nanovectors for tumor-selective gene delivery. *Technol. Cancer Res. Treat*. **4**(6):615–625 (2005).
115. G. Kaul, and M. Amiji. Biodistribution and targeting potential of poly(ethylene glycol)-modified gelatin nanoparticles in subcutaneous murine tumor model. *J. Drug Target*. **12**(9–10):585–591 (2004). doi:10.1080/10611860400013451.
116. T. Ameller, W. Marsaud, P. Legrand, R. Gref, and J. M. Renoir. *In vitro* and *in vivo* biologic evaluation of long-circulating biodegradable drug carriers loaded with the pure antiestrogen RU 58668. *Int. J. Cancer*. **106**(3):446–454 (2003). doi:10.1002/ijc.11248.
117. N. Benkirane, G. Guichard, J. P. Briand, and S. Muller. Exploration of requirements for peptidomimetic immune recognition—antigenic and immunogenic properties of reduced peptide bond pseudopeptide analogues of a histone hexapeptide. *J. Biol. Chem*. **271**(52):33218–33224 (1996). doi:10.1074/jbc.271.52.33218.
118. M. A. Babizhayev, Y. A. Semiletov, Y. A. Lul'kin, N. L. Sakina, E. L. Savel'yeva, L. M. Alimbarova, and I. P. Barinskii. 3D molecular modeling, free radical modulating and immune cells signaling activities of the novel peptidomimetic L-glutamyl-histamine: possible immunostimulating role. *Peptides*. **26** (4):551–563 (2005). doi:10.1016/j.peptides.2004.11.012.
119. J. A. Swanson, and A. D. Hoppe. The coordination of signaling during Fc receptor-mediated phagocytosis. *J. Leukocyte Biol*. **76** (6):1093–1103 (2004). doi:10.1189/jlb.0804439.
120. J. K. Czop. Phagocytosis of particulate activators of the alternative complement pathway: effects of fibronectin. *Adv. Immunol*. **38**:361–398 (1986). doi:10.1016/S0065-2776(08)60011-5.
121. D. Boyle, L. F. Tien, N. G. F. Cooper, V. Shepherd, and B. J. Mclaughlin. A mannose receptor is involved in retinal phagocytosis. *Invest. Ophthalmol. Vis. Sci*. **32**(5):1464–1470 (1991).
122. N. Murahashi, A. Sasaki, K. Higashi, A. Morikawa, and H. Yamada. Relationship between the anchor structure of the

galactosyl ligand for liposome modification and accumulation in the liver. *Biol. Pharm. Bull.* **18**(1):82–88 (1995).
123. S. Espuelas, P. Haller, F. Schuber, and B. Frisch. Synthesis of an amphiphilic tetraantennary mannosyl conjugate and incorporation into liposome carriers. *Bioorg. Med. Chem. Lett.* **13** (15):2557–2560 (2003). doi:10.1016/S0960-894X(03)00472-4.
124. C. D. Muller, and F. Schuber. Neo-mannosylated liposomes—synthesis and interaction with mouse Kupffer cells and resident peritoneal-macrophages. *Biochim. Biophys. Acta*. **986**(1):97–105 (1989). doi:10.1016/0005-2736(89)90277-0.
125. C. J. Cui, V. C. Stevens, and S. P. Schwendeman. Injectable polymer microspheres enhance immunogenicity of a contraceptive peptide vaccine. *Vaccine*. **25**(3):500–509 (2007). doi:10.1016/j.vaccine.2006.07.055.
126. A. Z. Wang, V. Bagalkot, C. C. Vasilliou, F. Gu, F. Alexis, L. Zhang, M. Shaikh, K. Yuet, C. M. J. R. Langer, P. W. Kantoff, N. H. Bander, S. Jon, and O. C. Farokhzad. Superparamagnetic iron oxide nanoparticle-aptamer bioconjugates for combined prostate cancer imaging and therapy. *ChemMedChem*. **3** (9):1311–1315 (2008). doi:10.1002/cmdc.200800091.
127. D. A. Mankoff, J. M. Link, H. M. Linden, L. Sundararajan, and K. A. Krohn. Tumor receptor imaging. *J. Nucl. Med*. **49**:149s–163s (2008). doi:10.2967/jnumed.107.045963.
128. S. Sofou, and G. Sgouros. Antibody-targeted liposomes in cancer therapy and imaging. *Expert Opin Drug Deliv*. **5** (2):189–204 (2008). doi:10.1517/17425247.5.2.189.
129. T. Kubota, S. Ikeda, and A. Okamoto. Intracellular mRNA imaging with a hybridization sensitive fluorescent nucleotide. *Nucleic Acids Symp. Ser.* **52**:355–356 (2008). doi:10.1093/nass/nrn179.
130. J. H. Kang, and J. K. Chung. Molecular-genetic imaging based on reporter gene expression. *J. Nucl. Med*. **49**:164s–179s (2008). doi:10.2967/jnumed.107.045955.
131. C. Rome, F. Couillaud, and C. T. W. Moonen. Gene expression and gene therapy imaging. *Eur. Radiol*. **17**(2):305–319 (2007). doi:10.1007/s00330-006-0378-z.
132. Y. W. Jun, J. H. Lee, and J. Cheon. Chemical design of nanoparticle probes for high-performance magnetic resonance imaging. *Angew. Chem. Int. Ed*. **47**(28):5122–5135 (2008). doi:10.1002/anie.200701674.
133. T. R. Pisanic, J. D. Blackwell, V. I. Shubayev, R. R. Finones, and S. Jin. Nanotoxicity of iron oxide nanoparticle internalization in growing neurons. *Biomaterials*. **28**(16):2572–2581 (2007). doi:10.1016/j.biomaterials.2007.01.043.
134. E. Chang, N. Thekkek, W. W. Yu, V. L. Colvin, and R. Drezek. Evaluation of quantum dot cytotoxicity based on intracellular uptake. *Small*. **2**(12):1412–1417 (2006). doi:10.1002/smll.200600218.
135. B. S. Kim, J. M. Qiu, J. P. Wang, and T. A. Taton. Magnetomicelles: composite nanostructures from magnetic nanoparticles and cross-linked amphiphilic block copolymers. *Nano Lett*. **5** (10):1987–1991 (2005). doi:10.1021/nl0513939.
136. N. Nasongkla, E. Bey, J. M. Ren, H. Ai, C. Khemtong, J. S. Guthi, S. F. Chin, A. D. Sherry, D. A. Boothman, and J. M. Gao. Multifunctional polymeric micelles as cancer-targeted, MRI-ultrasensitive drug delivery systems. *Nano Lett*. **6** (11):2427–2430 (2006). doi:10.1021/nl061412u.
137. A. L. Z. Lee, Y. Wang, W. H. Ye, H. S. Yoon, S. Y. Chan, and Y. Y. Yang. Efficient intracellular delivery of functional proteins using cationic polymer core/shell nanoparticles. *Biomaterials*. **29** (9):1224–1232 (2008). doi:10.1016/j.biomaterials.2007.11.021.
138. H. Toyama, K. Hatano, H. Suzuki, M. Ichise, S. Momosaki, G. Kudo, F. Ito, T. Kato, H. Yamaguchi, K. Katada, M. Sawada, and K. Ito. *In vivo* imaging of microglial activation using a peripheral benzodiazepine receptor ligand: [C-11]PK-11195 and animal PET following ethanol injury in rat striatum. *Ann. Nucl. Med*. **22**(5):417–424 (2008). doi:10.1007/s12149-008-0136-1.
139. M. P. Kung, C. Hou, B. P. Lieberman, S. Oya, D. E. Ponde, E. Blankemeyer, D. Skovronsky, M. R. Kilbourn, and H. F. Kung. *In vivo* imaging of beta-cell mass in rats using F-18-FP-(+)-DTBZ: a potential PET ligand for studying diabetes mellitus. *J. Nucl. Med*. **49**(7):1171–1176 (2008). doi:10.2967/jnumed.108.051680.
140. M. F. Bai, M. Sexton, N. Stella, and D. J. Bornhop. MBC94, a conjugable ligand for cannabinoid CB2 receptor imaging. *Bioconj. Chem*. **19**(5):988–992 (2008). doi:10.1021/bc700419e.
141. A. Biserni, F. Giannessi, A. F. Sciarroni, F. M. Milazzo, A. Maggi, and P. Ciana. *In vivo* imaging reveals selective peroxisome proliferator activated receptor modulator activity of the synthetic ligand 3-(1-(4-chlorobenzyl)-3-t-butylthio-5-isopropylindol-2-yl)-2,2-dimethylpropanoic acid (MK-886). *Mol. Pharmacol*. **73**(5):1434–1443 (2008). doi:10.1124/mol.107.042689.
142. N. Akhter, K. Shiba, K. Ogawa, S. Tsuji, S. Kinuya, K. Nakajima, and H. Mori. A change of *in vivo* characteristics depending on specific activity of radioiodinated (+)-2-[4-(4-iodophenyl)piperidino]cyclohexanol [(+)-pIV] as a ligand for sigma receptor imaging. *Nucl. Med. Biol*. **35**(1):29–34 (2008). doi:10.1016/j.nucmedbio.2007.09.005.
143. M. Bai, M. B. Rone, V. Papadopoulos, and D. J. Bornhop. A novel functional translocator protein ligand for cancer imaging. *Bioconj. Chem*. **18**(6):2018–2023 (2007). doi:10.1021/bc700251e.
144. N. Herold, K. Uebelhack, L. Franke, H. Amthauer, L. Luedemann, H. Bruhn, R. Felix, R. Uebelhack, and M. Plotkin. Imaging of serotonin transporters and its blockade by citalopram in patients with major depression using a novel SPECT ligand [I-123-ADAM. *J. Neural Transm.* **113**(5):659–670 (2006). doi:10.1007/s00702-005-0429-7.
145. Y. W. Jun, J. T. Jang, and J. Cheon. Magnetic nanoparticle assisted molecular MR imaging. *Bio-Appl. Nanoparticle*. **620**:85–106 (2007).
146. B. Stella, S. Arpicco, M. T. Peracchia, D. Desmaele, J. Hoebeke, M. Renoir, J. D'Angelo, L. Cattel, and P. Couvreur. Design of folic acid-conjugated nanoparticles for drug targeting. *J. Pharm. Sci*. **89**(11):1452–1464 (2000). doi:10.1002/1520-6017(200011)89:11<1452::AID-JPS8>3.0.CO;2-P.
147. B. Stella, V. Marsaud, S. Arpicco, G. Geraud, L. Cattel, P. Couvreur, and J. M. Renoir. Biological characterization of folic acid-conjugated poly(H(2)NPEGCA-co-HDCA) nanoparticles in cellular models. *J. Drug Target*. **15**(2):146–153 (2007). doi:10.1080/10611860600935826.
148. M. Candelaria, L. Taja-Chayeb, C. Arce-Salinas, S. Vidal-Millan, A. Serrano-Olvera, and A. Duenas-Gonzalez. Genetic determinants of cancer drug efficacy and toxicity: practical considerations and perspectives. *Anti-Cancer Drugs*. **16**(9):923–933 (2005). doi:10.1097/01.cad.0000180120.39278.c9.
149. Y. Chao, C. P. Li, T. Y. Chao, W. C. Su, R. K. Hsieh, M. F. Wu, K. H. Yeh, W. Y. Kao, L. T. Chen, and A. L. Cheng. An open, multi-centre, phase II clinical trial to evaluate the efficacy and safety of paclitaxel, UFT, and leucovorin in patients with advanced gastric cancer. *Br. J. Cancer*. **95**(2):159–163 (2006). doi:10.1038/sj.bjc.6603225.
150. Q. H. Zhao, B. S. Han, Z. H. Wang, C. Y. Gao, C. H. Peng, and J. C. Shen. Hollow chitosan-alginate multilayer microcapsules as drug delivery vehicle: doxorubicin loading and *in vitro* and *in vivo* studies. *Nanomed. Nanotechnol. Biol. Med*. **3**(1):63–74 (2007). doi:10.1016/j.nano.2006.11.007.
151. O. Gallego, and V. Puntes. What can nanotechnology do to fight cancer? *Clin. Transl. Oncol.* **8**:788–795 (2006). doi:10.1007/s12094-006-0133-6.
152. S. Modi, J. P. Jain, A. J. Domb, and N. Kumar. Exploiting EPR in polymer drug conjugate delivery for tumor targeting. *Current Pharmaceutical Design*. **12**(36):4785–4796 (2006). doi:10.2174/138161206779026272.
153. A. K. Iyer, G. Khaled, J. Fang, and H. Maeda. Exploiting the enhanced permeability and retention effect for tumor targeting. *Drug Discovery Today*. **11**(17–18):812–818 (2006). doi:10.1016/j.drudis.2006.07.005.
154. L. H. Reddy. Drug delivery to tumours: recent strategies. *J. Pharm. Pharmacol*. **57**(10):1231–1242 (2005). doi:10.1211/jpp.57.10.0001.
155. C. H. Heldin, K. Rubin, K. Pietras, and A. Ostman. High interstitial fluid pressure—an obstacle in cancer therapy. *Nat. Rev. Cancer*. **4**(10):806–813 (2004). doi:10.1038/nrc1456.
156. H. Maeda, J. Fang, T. Inutsuka, and Y. Kitamoto. Vascular permeability enhancement in solid tumor: various factors, mechanisms involved and its implications. *Int. Immunopharmacol*. **3**(3):319–328 (2003). doi:10.1016/S1567-5769(02)00271-0.
157. S. N. Ettinger, C. C. Poellmann, N. A. Wisniewski, A. A. Gaskin, J. S. Shoemaker, J. M. Poulson, M. W. Dewhirst, and B. KLitzman. Urea as a recovery marker for quantitative assessment of tumor interstitial solutes with microdialysis. *Cancer Res*. **61**(21):7964–7970 (2001).

158. T. D. Harris, S. Kalogeropoulos, T. Nguyen, S. Liu, J. Bartis, C. Ellars, S. Edwards, D. Onthank, P. Silva, P. Yalamanchili, S. Robinson, J. Lazewatsky, J. Barrett, and J. Bozarth. Design, synthesis, and evaluation of radiolabeled integrin alpha(v)beta (3) receptor antagonists for tumor imaging and radiotherapy. *Cancer Biother. Radiopharm.* **18**(4):627–641 (2003). doi:10.1089/108497803322287727.
159. C.-Y. Ke, C. Mathias, and M. Green. The folate receptor as a molecular model for tumor-selective radionuclide delivery. *Nuclear Med. Biol.* **30**:811–817 (2003). doi:10.1016/S0969-8051(03)00117-3.
160. L. Brannon-Peppas, and J. O. Blanchette. Nanoparticle and targeted systems for cancer therapy. *Adv. Drug Deliv. Rev.* **56**(11):1649–1659 (2004). doi:10.1016/j.addr.2004.02.014.
161. X. B. B. Zhao, and R. J. Lee. Tumor-selective targeted delivery of genes and antisense oligodeoxyribonucleotides via the folate receptor. *Adv. Drug Deliv. Rev.* **56**(8):1193–1204 (2004). doi:10.1016/j.addr.2004.01.005.
162. L. J. Yang, J. Li, W. Zhou, X. Yuan, and S. Li. Targeted delivery of antisense oligodeoxynucleotides to folate receptor-overexpressing tumor cells. *J. Contr. Rel.* **95**(2):321–331 (2004).
163. Y. Y. Jiang, C. Liu, M. H. Hong, S. J. Zhu, and Y. Y. Pei. Tumor cell targeting of transferrin-PEG-TNF-alpha conjugate via a receptor-mediated delivery system: design, synthesis, and biological evaluation. *Bioconj. Chem.* **18**(1):41–49 (2007). doi:10.1021/bc060135f.
164. D. Bar, R. N. Apte, E. Voronov, C. A. Dinarello, and S. Cohen. A continuous delivery system of IL-1 receptor antagonist reduces angiogenesis and inhibits tumor development. *FASEB J.* **18**(1):161–163 (2003).
165. C. Mamot, D. C. Drummond, U. Greiser, K. Hong, D. B. Kirpotin, J. D. Marks, and J. W. Park. Epidermal growth factor receptor (EGFR)-targeted immunoliposomes mediate specific and efficient drug delivery to EGFR- and EGFRvIII-overexpressing tumor cells. *Cancer Res.* **63**(12):3154–3161 (2003).
166. C. M. Huang, Y. T. Wu, and S. T. Chen. Targeting delivery of paclitaxel into tumor cells via somatostatin receptor endocytosis. *Chem. Biol.* **7**(7):453–461 (2000). doi:10.1016/S1074-5521(00)00131-9.
167. G. Mariani, P. A. Erba, and A. Signore. Receptor-mediated tumor targeting with radiolabeled peptides: there is more to it than somatostatin analogs. *J. Nucl. Med.* **47**(12):1904–1907 (2006).
168. S. R. Li, E. Koller, P. Valent, D. Gludovacz, Q. Yang, P. Patri, P. Angelberger, R. Dudczak, and I. Virgolini. Effects of vasoactive intestinal peptide (VIP) and somatostatin (SST) on lipoprotein receptor expression by A431 tumor cells. *Life Sci.* **68**(11):1243–1257 (2001). doi:10.1016/S0024-3205(00)01023-7.
169. B. A. Nock, T. Maina, M. Behe, A. Nikolopoulou, M. Gotthardt, J. S. Schmitt, T. M. Behr, and H. R. Macke. CCK-2/gastrin receptor-targeted tumor imaging with Tc-99m-labeled minigastrin analogs. *J. Nucl. Med.* **46**(10):1727–1736 (2005).
170. M. de Visser, W. M. van Weerden, C. M. A. de Ridder, S. Reneman, M. Melis, E. P. Krenning, and M. de Jong. Androgen-dependent expression of the gastrin-releasing peptide receptor in human prostate tumor xenografts. *J. Nucl. Med.* **48**(1):88–93 (2007).
171. C. Haase, R. Bergmann, J. Oswald, D. Zips, and J. Pietzsch. Neurotensin receptors in adeno- and squamous cell carcinoma. *Anticancer Res.* **26**(5A):3527–3533 (2006).
172. K. Podar, G. Tonon, M. Sattler, Y. T. Tai, S. LeGouill, H. Yasui, K. Ishitsuka, R. Kumar, L. N. Pandite, T. Hideshima, D. Chauhan, and K. C. Anderson. The small-molecule VEGF-receptor inhibitor pazopanib (GW786034B) targets both tumor and endothelial cells in multiple myeloma. *Blood.* **108**(11):339B–339B (2006).
173. T. S. Udayakumar, E. L. Bair, R. B. Nagle, and G. T. Bowden. Pharmacological inhibition of FGF receptor signaling inhibits LNCaP prostate tumor growth, promatrilysin, and PSA expression. *Mol. Carcinog.* **38**(2):70–77 (2003). doi:10.1002/mc.10146.
174. R. M. Owen, C. B. Carlson, J. W. Xu, P. Mowery, E. Fasella, and L. L. Kiessling. Bifunctional ligands that target cells displaying the alpha(v)beta(3) integrin. *ChemBioChem.* **8**(1):68–82 (2007). doi:10.1002/cbic.200600339.
175. C. B. Carlson, P. Mowery, R. M. Owen, E. C. Dykhuizen, and L. L. Kiessling. Selective tumor cell targeting using low-affinity, multivalent interactions. *ACS Chem. Biol.* **2**(2):119–127 (2007). doi:10.1021/cb6003788.
176. A. M. Lillo, C. Z. Sun, C. S. Gao, H. Ditzel, J. Parrish, C. M. Gauss, J. Moss, B. Felding-Habermann, P. Wirsching, D. L. Boger, and K. D. Janda. A human single-chain antibody specific for integrin alpha(3)beta(1) capable of cell internalization and delivery of antitumor agents. *Chem. Biol.* **11**(7):897–906 (2004). doi:10.1016/j.chembiol.2004.04.018.
177. B. Felding-Habermann. Integrin adhesion receptors in tumor metastasis. *Clin. Exp. Metastasis.* **20**(3):203–213 (2003). doi:10.1023/A:1022983000355.
178. P. Lanza, B. FeldingHabermann, Z. M. Ruggeri, M. Zanetti, and R. Billetta. Selective interaction of a conformationally-constrained Arg-Gly-Asp (RGD) motif with the integrin receptor alpha nu beta 3 expressed on human tumor cells. *Blood Cells Mol. Dis.* **23**(12):230–241 (1997). doi:10.1006/bcmd.1997.0140.
179. X. He, and E. Jabbari. Solid-phase synthesis of reactive peptide crosslinker by selective deprotection. *Protein Pept. Lett.* **13**(7):715–718 (2006). doi:10.2174/092986606777790610.
180. S. Moore. Facilitating oral chemotherapy treatment and compliance through patient/family-focused education. *Cancer Nursing.* **30**(2):112–122 (2007). doi:10.1097/01.NCC.0000265009.33053.2d.
181. M. K. Danks, K. J. Yoon, R. A. Bush, J. S. Remack, M. Wierdl, L. Tsurkan, S. U. Kim, E. Garcia, M. Z. Metz, J. Najbauer, P. M. Potter, and K. S. Aboody. Tumor-targeted enzyme/prodrug therapy mediates long-term disease-free survival of mice bearing disseminated neuroblastoma. *Cancer Res.* **67**(1):22–25 (2007). doi:10.1158/0008-5472.CAN-06-3607.
182. D. Ravel, V. Dubois, J. Quinonero, F. Meyer-Losic, J. P. Delord, P. Rochaix, C. Nicolazzi, F. Ribes, C. Mazerolles, E. Assouly, K. Vialatte, I. Hor, J. Kearsey, and A. Trouet. Preclinical toxicity, toxicokinetics, and antitumoral efficacy studies of DTS-201, a tumor-selective peptidic prodrug of doxorubicin. *Clin. Cancer Res.* **14**(4):1258–1265 (2008). doi:10.1158/1078-0432.CCR-07-1165.
183. Y. Yoneda, S. Steiniger, K. Capková, J. M. Mee, Y. Liu, G. F. Kaufmann, and K. D. Janda. A cell-penetrating peptidic GRP78 ligand for tumor cell-specific prodrug therapy. *Bioorg. Med. Chem. Lett.* **18**(5):1632–1636 (2008). doi:10.1016/j.bmcl.2008.01.060.
184. S. Zalipsky, M. Saad, R. Kiwan, E. Ber, N. Yu, and T. Minko. Antitumor activity of new liposomal prodrug of mitomycin C in multidrug resistant solid tumor: insights of the mechanism of action. *J. Drug Target.* **15**(7–8):518–530 (2007). doi:10.1080/10611860701499946.
185. A. S. Lalani, S. E. Alters, A. Wong, M. R. Albertella, J. L. Cleland, and W. D. Henner. Selective tumor targeting by the hypoxia-activated prodrug AQ4N blocks tumor growth and metastasis in preclinical models of pancreatic cancer. *Clin. Cancer Res.* **13**(7):2216–2225 (2007). doi:10.1158/1078-0432.CCR-06-2427.
186. W. Wu, Y. Luo, C. Sun, Y. Liu, P. Kuo, J. Varga, R. Xiang, R. Reisfeld, K. D. Janda, T. S. Edgington, and C. Liu. Targeting cell-impermeable prodrug activation to tumor microenvironment eradicates multiple drug-resistant neoplasms. *Cancer Res.* **66**(2):970–980 (2006). doi:10.1158/0008-5472.CAN-05-2591.
187. G. Schwarz, J. Brandenburg, M. Reich, T. Burster, C. Driessen, and H. Kalbacher. Characterization of legumain. *Biol. Chem.* **383**(11):1813–1816 (2002). doi:10.1515/BC.2002.203.
188. C. Liu, C. Z. Sun, H. N. Huang, K. Janda, and T. Edgington. Overexpression of legumain in tumors is significant for invasion/metastasis and a candidate enzymatic target for prodrug therapy. *Cancer Res.* **63**(11):2957–2964 (2003).
189. J. Gawenda, F. Traub, H. J. Luck, H. Kreipe, and R. von Wasielewski. Legumain expression as a prognostic factor in breast cancer patients. *Breast Cancer Res Treat.* **102**(1):1–6 (2007). doi:10.1007/s10549-006-9311-z.
190. S. Lewen, H. Zhou, H. D. Hu, T. M. Cheng, D. Markowitz, R. A. Reisfeld, R. Xiang, and Y. P. Luo. A Legumain-based minigene vaccine targets the tumor stroma and suppresses breast cancer growth and angiogenesis. *Cancer Immunol. Immunother.* **57**(4):507–515 (2008). doi:10.1007/s00262-007-0389-x.
191. C. M. Berger, K. L. Knutson, L. G. Salazar, S. K., and M. L. Disis. Peptide-based vaccines. 2002. http://depts.washington.

edu/tumorvac/MultiMedia/Publications/PeptideBasedVaccines-2002.pdf.
192. L. Florea, B. Hallorsson, O. Kohlbacher, R. Schwartz, S. Hoffman, and S. Istrail. Epitope prediction algorithms for peptide-based vaccine design. Proceedings of the IEEE Computer Society Bioinformatics Conference 2003.
193. A. Pashov, B. Monzavi-Karbassi, G. Raghava, and T. Kieber-Emmons. Peptide mimotopes as prototypic templates of broad-spectrum surrogates of carbohydrate antigens for cancer vaccination. *Crit. Rev. Immunol.* **27**(3):247–270 (2007).
194. A. B. Nesburn, X. Zhang, A. Issagholian, X. Zhu, and L. BenMohamed. Induction of CD8 T-cell-specific immunity against ocular herpes simplex virus with a Th-CTL fusion synthetic lipopeptide: the lipid moiety units influence priming for protective $CD8^+$ cytotoxic T lymphocytes. *Invest. Ophthalmol. Vis. Sci.* **46**:15289–15301 (2005).
195. C. Mesa, and L. E. Fernandez. Challenges facing adjuvants for cancer immunotherapy. *Immunol. Cell Biol.* **82**(6):644–650 (2004). doi:10.1111/j.0818-9641.2004.01279.x.
196. M. A. Sommerfelt, and B. Sorensen. Prospects for HIV-1 therapeutic immunisation and vaccination: the potential contribution of peptide immunogens. *Expert Opin. Biol. Ther.* **8**(6):745–757 (2008). doi:10.1517/14712598.8.6.745.
197. C. S. Klade, H. Wedemeyer, T. Berg, H. Hinrichsen, G. Cholewinska, S. Zeuzem, H. Blum, M. Buschle, S. Jelovcan, V. Buerger, E. Tauber, J. Frisch, and M. P. Manns. Therapeutic vaccination of chronic hepatitis c nonresponder patients with the peptide vaccine IC41. *Gastroenterology.* **134**(5):1385–1395 (2008). doi:10.1053/j.gastro.2008.02.058.
198. H. Takahashi, H. Ishizaki, H. Tahara, Y. Tamaki, and Y. Yanagi. Suppression of choroidal neovascularization by vaccination with epitope peptide derived from human VEGF receptor 2 in an animal model. *Invest. Ophthalmol. Vis. Sci.* **49**(5):2143–2147 (2008). doi:10.1167/iovs.07-0523.
199. E. G. Marazuela, N. Prado, E. Morow, H. Fernandez-Garcia, M. Villalba, R. Rodriguez, and E. Batanero. Intranasal vaccination with poly(lactide-co-glycolide) microparticles containing a peptide T of Ole e 1 prevents mice against sensitization. *Clin. Exp. Allergy.* **38**(3):520–528 (2008). doi:10.1111/j.1365-2222.2007.02922.x.
200. R. Glück, K. G. Burri, and I. Metcalfe. Adjuvant and antigen delivery properties of virosomes. *Curr. Drug Del.* **2**(4):395–400 (2005). doi:10.2174/156720105774370302.
201. H. J. Peng, L. C. Tsai, S. N. Su, Z. N. Chang, H. D. Shen, P. L. Chao, S. W. Kuo, I. Y. Tsao, and M. W. Hung. Comparison of different adjuvants of protein and DNA vaccination for the prophylaxis of IgE antibody formation. *Vaccine.* **22**(5–6):755–761 (2004). doi:10.1016/j.vaccine.2003.08.030.
202. S. K. Kim, G. Ragupathi, C. Musselli, S. J. Choi, Y. S. Park, and P. O. Livingston. Comparison of the effect of different immunological adjuvants on the antibody and T-cell response to immunization with MUC1-KLH and GD3-KLH conjugate cancer vaccines. *Vaccine*. **18**(7–8):597–603 (1999). doi:10.1016/S0264-410X(99)00316-3.
203. S. Hoshi, A. Uchino, N. Saito, K. I. Kusanagi, T. Ihara, and S. Ueda. Comparison of adjuvants with respect to serum IgG antibody response in orally immunized chickens. *Comp. Immunol. Microbiol. Infect. Dis*. **22**(1):63–69 (1999). doi:10.1016/S0147-9571(98)00017-4.
204. H. Tamber, P. Johansen, H. P. Merkle, and B. Gander. Formulation aspects of biodegradable polymeric microspheres for antigen delivery. *Adv. Drug Del. Rev.* **57**(3):357–376 (2005). doi:10.1016/j.addr.2004.09.002.
205. Y. Waeckerle-Men, and M. Groettrup. PLGA microspheres for improved antigen delivery to dendritic cells as cellular vaccines. *Adv. Drug Del. Rev.* **57**(3):475–482 (2005). doi:10.1016/j.addr.2004.09.007.
206. A. Luzardo-Alvarez, N. Blarer, K. Peter, J. F. Romero, C. Reymond, G. Corradin, and B. Gander. Biodegradable microspheres alone do not stimulate murine macrophages *in vitro*, but prolong antigen presentation by macrophages *in vitro* and stimulate a solid immune response in mice. *J. Contr. Rel.* **109**(1–3):62–76 (2005). doi:10.1016/j.jconrel.2005.09.015.
207. Y. Waeckerle-Men, E. Scandella, E. U. Allmen, B. Ludewig, S. Gillessen, H. P. Merkle, B. Gander, and M. Groettrup. Phenotype and functional analysis of human monocyte-derived dendritic cells loaded with biodegradable poly(lactide-co-glycolide) microspheres for immunotherapy. *J. Immunol. Methods*. **287**(1–2):109–124 (2004). doi:10.1016/j.jim.2004.01.010.
208. M. Amidi, S. G. Romeijn, J. C. Verhoef, H. E. Junginger, L. Bungener, A. Huckriede, D. J. A. Crommelin, and W. Jiskoot. *N*-Trimethyl chitosan (TMC) nanoparticles loaded with influenza subunit antigen for intranasal vaccination: biological properties and immunogenicity in a mouse model. *Vaccine*. **25**(1):144–153 (2007). doi:10.1016/j.vaccine.2006.06.086.
209. T. Yoshikawa, N. Okada, A. Oda, K. Matsuo, K. Matsuo, H. Kayamuro, Y. Ishii, T. Yoshinaga, T. Akagi, M. Akashi, and S. Nakagawa. Nanoparticles built by self-assembly of amphiphilic gamma-PGA can deliver antigens to antigen-presenting cells with high efficiency: a new tumor-vaccine carrier for eliciting effector T cells. *Vaccine*. **26**(10):1303–1313 (2008). doi:10.1016/j.vaccine.2007.12.037.
210. S. Hamdy, P. Elamanchili, A. Alshamsan, O. Molavi, T. Satou, and J. Samuel. Enhanced antigen-specific primary CD4(+) and CD8(+) responses by codelivery of ovalbumin and toll-like receptor ligand monophosphoryl lipid A in poly(D,L-lactic-co-glycolic acid) nanoparticles. *J. Biomed. Mater. Res. A*. **81A**(3):652–662 (2007). doi:10.1002/jbm.a.31019.
211. S. Lisi, R. Peterkova, M. Peterka, J. L. Vonesch, J. V. Ruch, and H. Lesot. Tooth morphogenesis and pattern of odontoblast differentiation. *Connect. Tissue Res*. **44**:167–170 (2003). doi:10.1080/713713612.
212. U. Ripamonti, and A. H. Reddi. Tissue engineering, morphogenesis, and regeneration of the periodontal tissues by bone morphogenetic proteins. *Crit. Rev. Oral Biol. Med*. **8**(2):154–163 (1997).
213. Y. Robinson, C. E. Heyde, S. K. Tschoke, M. A. Mont, T. M. Seyler, and S. D. Ulrich. Evidence supporting the use of bone morphogenetic proteins for spinal fusion surgery. *Exp. Rev. Med. Dev*. **5**(1):75–84 (2008). doi:10.1586/17434440.5.1.75.
214. J. M. Wozney. Overview of bone morphogenetic proteins. *Spine*. **27**(16 Suppl 1):S2–S8 (2002). doi:10.1097/00007632-200208151-00002.
215. B. McKay, and H. S. Sandhu. Use of recombinant human bone morphogenetic protein-2 in spinal fusion applications. *Spine*. **27**(16 Suppl 1):S66–S85 (2002). doi:10.1097/00007632-200208151-00014.
216. R. A. Meyer Jr., M. H. Meyer, M. Tenholder, S. Wondracek, R. Wasserman, and P. Garges. Gene expression in older rats with delayed union of femoral fractures. *J. Bone Jt. Surg. (Am.)*. **85-A**(7):1243–1254 (2003).
217. K. Behnam, M. L. Phillips, J. D. Silva, E. J. Brochmann, M. E. Duarte, and S. S. Murray. BMP binding peptide: a BMP-2 enhancing factor deduced from the sequence of native bovine bone morphogenetic protein/non-collagenous protein. *J. Orthop. Res*. **23**(1):175–180 (2005). doi:10.1016/j.orthres.2004.05.001.
218. F. Hillger, G. Herr, R. Rudolph, and E. Schwarz. Biophysical comparison of BMP-2, ProBMP-2, and the free pro-peptide reveals stabilization of the pro-peptide by the mature growth factor. *J. Biol. Chem*. **280**(15):14974–14980 (2005). doi:10.1074/jbc.M414413200.
219. X. Lin, P. O. Zamora, S. Albright, J. D. Glass, and L. A. Pena. Multidomain synthetic peptide B2A2 synergistically enhances BMP-2 *in vitro*. *J. Bone Miner. Res*. **20**(4):693–703 (2005). doi:10.1359/JBMR.041104.
220. L. B. E. Shields, G. H. Raque, S. D. Glassman, M. Campbell, T. Vitaz, J. Harpring, and C. B. Shields. Adverse effects associated with high-dose recombinant human bone morphogenetic protein-2 use in anterior cervical spine fusion. *Spine*. **31**(5):542–547 (2006). doi:10.1097/01.brs.0000201424.27509.72.
221. J. B. Oldham, L. Lu, X. Zhu, B. D. Porter, T. E. Hefferan, D. R. Larson, B. L. Currier, A. G. Mikos, and M. J. Yaszemski. Biological activity of rhBMP-2 released from PLGA microspheres. *J. Biomech. Eng. Trans. ASME*. **122**(3):289–292 (2000). doi:10.1115/1.429662.
222. M. C. Meikle. On the transplantation, regeneration and induction of bone: the path to bone morphogenetic proteins and other skeletal growth factors. *Surg.: J. R. Coll. Surg. Edinb. Ir.* **5**(4):232–243 (2007).
223. K. C. Klein, J. C. Reed, and J. R. Lingappa. Intracellular destinies: degradation, targeting, assembly, and endocytosis of HIV Gag. *AIDS Rev.* **9**(3):150–610 (2007).
224. M. Amyere, M. Mettlen, P. Van der Smissen, A. Platek, B. Payrastre, A. Veithen, and P. J. Courtoy. Origin, originality, functions, subversions and molecular signalling of macropino-

cytosis. *Int. J. Med. Microbiol*. **291**(6–7):487–494 (2002). doi:10.1078/1438-4221-00157.
225. J. Z. Rappoport. Focusing on clathrin-mediated endocytosis. *Biochem. J*. **412**:415–423 (2008). doi:10.1042/BJ20080474.
226. L. Pelkmans. Secrets of caveolae- and lipid raft-mediated endocytosis revealed by mammalian viruses. *Biochim. Biophys. Acta Mol. Cell Res*. **1746**(3):295–304 (2005). doi:10.1016/j.bbamcr.2005.06.009.
227. D. Holler, and I. Dikic. Receptor endocytosis via ubiquitin-dependent and -independent pathways. *Biochem. Pharmacol*. **67**(6):1013–1017 (2004). doi:10.1016/j.bcp.2004.01.003.
228. M. A. McNiven. Big gulps: specialized membrane domains for rapid receptor-mediated endocytosis. *Trends Cell Biol*. **16** (10):487–492 (2006). doi:10.1016/j.tcb.2006.08.007.
229. S. H. Kim, J. H. Jeong, K. W. Chun, and T. G. Park. Target-specific cellular uptake of PLGA nanoparticles coated with poly (L-lysine)-poly(ethylene glycol)-folate conjugate. *Langmuir*. **21** (19):8852–8857 (2005). doi:10.1021/la0502084.
230. J. P. Luzio, B. A. Rous, N. A. Bright, P. R. Pryor, B. M. Mullock, and R. C. Piper. Lysosome–endosome fusion and lysosome biogenesis. *J. Cell Sci*. **113**(9):1515–1524 (2000).
231. K. Sasaki, K. Kogure, S. Chaki, Y. Nakamura, R. Moriguchi, H. Hamada, R. Danev, K. Nagayama, S. Futaki, and H. Harashima. An artificial virus-like nano carrier system: enhanced endosomal escape of nanoparticles via synergistic action of pH-sensitive fusogenic peptide derivatives. *Anal. Bioanal. Chem*. **391**(8):2717–2727 (2008). doi:10.1007/s00216-008-2012-1.
232. K. M. Stewart, K. L. Horton, and S. O. Kelley. Cell-penetrating peptides as delivery vehicles for biology and medicine. *Org. Biomol. Chem*. **6**(13):2242–2255 (2008). doi:10.1039/b719950c.
233. M. E. Herbig, K. M. Welter, and H. A. Merkle. Reviewing biophysical and cell biological methodologies in cell-penetrating peptide (CPP) research. *Crit. Rev. Ther. Drug Carr. Sys*. **24** (3):203–255 (2007).
234. M. C. Morris, S. Deshayes, F. Heitz, and G. Divita. Cell-penetrating peptides: from molecular mechanisms to therapeutics. *Biol. Cell*. **100**(4):201–217 (2008). doi:10.1042/BC20070116.
235. C. Foerg, and H. P. Merkle. On the biomedical promise of cell penetrating peptides: limits *versus* prospects. *J. Pharm. Sci*. **97** (1):144–162 (2008). doi:10.1002/jps.21117.
236. P. Jarvert, K. Langel, S. El-Andaloussi, and U. Langel. Applications of cell-penetrating peptides in regulation of gene expression. *Biochem. Soc. Trans*. **35**:770–774 (2007). doi:10.1042/BST0350770.
237. J. S. Suk, J. Suh, K. Choy, S. K. Lai, J. Fu, and J. Hanes. Gene delivery to differentiated neurotypic cells with RGD and HIV Tat peptide functionalized polymeric nanoparticles. *Biomaterials*. **27**(29):5143–5150 (2006). doi:10.1016/j.biomaterials.2006.05.013.